Glow Discharge Optical Spectroscopy and Mass Spectrometry

Annemie Bogaerts

Research group PLASMANT, University of Antwerp, Wilrijk-Antwerp, Belgium

Atomic Spectroscopy Optical (atomic absorption spectroscopy, AAS; atomic emission spectroscopy, AES; atomic fluorescence spectroscopy, AFS; and optogalvanic spectroscopy) and mass spectrometric (magnetic sector, quadrupole mass analyzer, QMA; quadrupole ion trap, QIT; Fourier transform ion cyclotron resonance, FTICR; and time-of-flight, TOF) instrumentation are well suited for coupling to the glow discharge (GD).

The GD is a relatively simple device. A potential gradient (500–1500 V) is applied between an anode and a cathode. In most cases, the sample is also the cathode. A noble gas (mostly Ar) is introduced into the discharge region before power initiation. When a potential is applied, electrons are accelerated toward the anode. As these electrons accelerate, they collide with gas atoms. A fraction of these collisions are of sufficient energy to remove an electron from a support gas atom, forming an ion. These ions are, in turn, accelerated toward the cathode. These ions impinge on the surface of the cathode, sputtering sample atoms from the surface. Sputtered atoms that do not redeposit on the surface diffuse into the excitation/ionization regions of the plasma where they can undergo excitation and/or ionization via a number of collisional processes, and the photons or ions created in this way can be detected with optical emission spectroscopy or mass spectrometry.

GD sources offer a number of distinct advantages that make them well suited for specific types of analyses. These sources afford direct analysis of solid samples, thus minimizing the sample preparation required for analysis. The nature of the plasma also provides mutually exclusive atomization and excitation processes that help to minimize the matrix effects that plague so many other elemental techniques. In recent years, there is also increasing interest for using GD sources for liquid and gas analyses.

In this article, first, the principles of operation of the GD plasma are reviewed, with an emphasis on how those principles relate to optical spectroscopy and mass spectrometry. Basic applications of the GD techniques are considered next. These include bulk analysis, surface analysis, and the analysis of solution and gaseous samples. The requirements necessary to obtain optical information are addressed following the analytical applications. This article focuses on the instrumentation needed to make optical measurements using the GD as an atomization/excitation source. Finally, mass spectrometric instrumentation and interfaces are addressed as they pertain to the use of a GD plasma as an ion source. GD sources provide analytically useful gas-phase species from solid samples. These sources can be interfaced with a variety of spectroscopic and spectrometric instruments for both quantitative and qualitative analyses.

1 INTRODUCTION

We have always questioned the physical makeup of our universe, but only recently has science advanced to the point that some of the most fundamental questions can be answered. Although all fields of science play a role

Update based on the original article by Robert E. Steiner and Christopher M. Barshick, Encyclopedia of Analytical Chemistry, ©2000, John Wiley & Sons, Ltd

Encyclopedia of Analytical Chemistry, Online © 2006–2016 John Wiley & Sons, Ltd.

This article was published in the *Encyclopedia of Analytical Chemistry* in 2016 by John Wiley & Sons, Ltd.
DOI: 10.1002/9780470027318.a5107.pub3

in information gathering, this is the specific charge of the analytical chemist. The field of analytical chemistry is broad, and although no one area can claim to be more valuable than another, the area of elemental analysis has always been critical to our understanding of the chemical and physical properties of materials.

Many years ago, chemists characterized the world in terms of the basic elements such as fire, earth, air, and water. Today, we classify our world in a similar manner, but in terms of carbon, nitrogen, oxygen, hydrogen, and so on; all that has really changed are the techniques we use – techniques that allow us to measure elemental and isotopic composition, elemental speciation, and spatial distribution of atoms and molecules.

This article focuses on two techniques used in elemental analysis: GD optical and mass spectrometries. We begin by describing the fundamental operation of a GD, including the sputtering and ionization processes. Next, we examine optical techniques that take advantage of the GD as an atomization source. Finally, we conclude by describing GD mass spectrometry, a powerful tool for multielement ultratrace analysis.

2 THE GLOW DISCHARGE

Although not always apparent, aspects of our everyday lives are permeated with technologies originally developed to solve scientific problems. An excellent example is the GD. Developed in the early twentieth century[1–3] as a spectrochemical ionization source used for fundamental studies of atomic structure, a variation of the same GD now illuminates storefronts in the guise of the common neon sign. Moreover, it is used for the deposition of coatings and the fabrication of integrated circuits in the microelectronics industry, forms the basis of plasma TVs, and finds increasing applications in environmental and biomedical fields.[4]

The GD is a simple device. Before delving into the fundamental processes that characterize the glow, however, it is useful to define a few terms. A GD is an example of a general class of excitation/ionization sources known as 'plasmas'. This term refers to a partially ionized gas with equal numbers of positive and negative species (ions or electrons) and a larger number of neutral species.[5] A GD is a simple form of a gas discharge. A gas discharge is formed by passing an electric current through a gaseous medium.[6] For current to flow through this medium, a fraction of the gas must be ionized. In its simplest form, one applies a potential gradient between a cathode and an anode; in doing so, electrons are accelerated toward the anode. As the electrons move through the gas, they collide with gas-phase atoms. A fraction of these collisions will be of sufficient energy to remove an electron from an atom, thus producing an ion and a secondary electron. The positively charged gas ions will, in turn, be accelerated toward and impinge upon the negatively biased sample cathode. Upon impact a variety of species will be liberated from the surface. Gas-phase sample atoms are then free to diffuse into the plasma where they can undergo excitation and ionization. These dynamic processes are depicted in Figure 1.

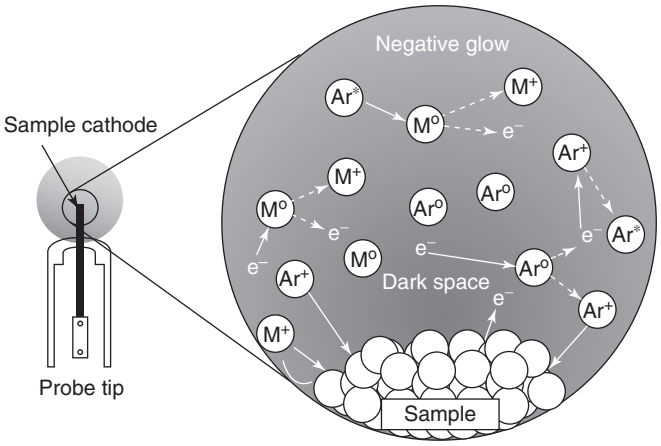

Figure 1 Illustration of various steady-state plasma processes. (Reproduced with permission from Ref. 7. © John Wiley & Sons, Ltd., 1995.)

A GD can be formed in virtually any vacuum cell that can be equipped with an inlet for a support gas. A variety of geometries have been investigated in the past. Table 1 lists some of the most common GD ion sources and their characteristics. A very popular source is based on a cross-shaped vacuum housing that provides ports for spectroscopic viewing, sample introduction, gas introduction, pressure monitoring, and ion extraction. The most widely used commercial source, mainly for optical emission spectrometry but more recently also for mass spectrometry, is the so-called Grimm source[8] and derivations of it.

2.1 Fundamental Glow Discharge Processes

The fundamental processes occurring in the discharge define a number of discrete regions. In this article, only three regions – the cathode dark space, the negative glow, and the anode region – are defined, because the other regions, although important, are often not visible owing to limited separation of the cathode and anode. For a complete treatise on this subject, the reader is directed to several excellent articles.[9–11] The cathode dark space is characterized by low-light intensity relative to other regions of the plasma. This lack of luminosity arises from the absence of collisions and consequently

Encyclopedia of Analytical Chemistry, Online © 2006–2016 John Wiley & Sons, Ltd.

This article was published in the *Encyclopedia of Analytical Chemistry* in 2016 by John Wiley & Sons, Ltd.
DOI: 10.1002/9780470027318.a5107.pub3

Table 1 GD ion sources and their characteristics

	Voltage (V)	Current (mA)	Pressure (Torr)	Advantages	Disadvantages
Coaxial cathode	800–1500	1–5	0.1–10	Can conform to various sample shapes and sizes Penning ionization dominated	Powders must be pressed
Grimm	500–1000	25–100	1–5	Depth profiling Compacted powder samples	Flat samples only High gas flow rates
Hollow cathode	200–500	10–100	0.1–10	High sputter rate Intense ion beams for mass spectrometry Large localized atom populations for optical spectroscopy	Complicated geometry Charge exchange mechanism is important
Jet enhanced	800–1000	25–30	1–5	High sputter rate Compacted powder samples	Flat samples only High gas flow rates

the absence of excitation and the radiative relaxation events that produce photons. The cathode dark space is located between the cathode surface and the negative glow region. The presence of a large positive space charge in the cathode dark space causes the development of a potential gradient. The bulk discharge potential decreases rapidly through this region, leading to its common name, the *cathode fall*. This large potential gradient affects the acceleration of electrons that can ionize the discharge gas species and liberate secondary electrons in the negative glow,[5] which help to sustain the plasma. Radiative relaxation of species excited in the negative glow region yields the characteristic emission for which it is named. There is nearly charge neutrality (equal positive and negative charges) in this region, but the major charge carriers in this region are electrons, because of their higher mobility. As electrons collisionally cool, they slow down, decreasing their cross-section for excitational collisions with atoms. This smaller excitation cross-section can result in the Faraday dark space close to the anode, but when the distance between the cathode and anode is small, like in most GDs used for analytical applications, the Faraday dark space is not visible, and there is only a small anode region, where the potential returns to zero. Figure 2 schematically shows these three regions, as well as the potential and electric field distributions, positive ion and electron densities, and electron impact excitation rate (which corresponds roughly to the light intensity) in these regions, as obtained from model calculations.[12]

2.1.1 The Sputtering Process

The GD is of particular utility when analyzing solid conducting samples. Most competing techniques used for elemental applications (i.e. inductively coupled plasma mass spectrometry [ICPMS], flame spectroscopies, and graphite furnace techniques) require a sample in solution form to facilitate aspiration or introduction into the ionization source. The GD source possesses the inherent characteristic of producing gas-phase analyte atoms directly from the solid conducting sample material. This phenomenon, known simply as *cathodic sputtering*, can be most easily described using a basic billiard ball analogy. Positively charged discharge gas ions are accelerated toward the negatively biased sample cathode. Before impact, these high-energy ions recombine with Auger electrons released from the cathode surface. The resulting high-energy neutral species impact the surface of the cathode, transforming their kinetic energy (KE) into the lattice of the sample, thus causing a cascade of collisional events, much like the breaking of a racked set of billiard balls. If the resulting energy transfer is sufficient to overcome a surface atom's binding energy, the atom will be released into the gas phase. The sputtering process liberates not only individual cathodic atoms but also electrons, ions, and clusters of atoms and molecules. This process is illustrated in Figure 3.

Emitted electrons are accelerated across the cathode dark space into the negative glow where they can contribute to excitation and ionization of gas-phase atoms. The ions formed by the sputtering event do not travel far from the cathode but are returned to the surface by the effects of the electric field. Once in the gas phase, the analyte atoms and neutral clusters are free to undergo collisions that may dissociate clusters and redeposit atoms at the surface. A fraction of these neutrals diffuse into the negative glow where they undergo excitation/ionization.

The effect of an ion's impact on the sample lattice can be measured by the sputter yield, S, as shown in Equation (1)[13]:

$$S = (9.6 \times 10^4)\left(\frac{W}{M} i^+ t\right) \quad (1)$$

Encyclopedia of Analytical Chemistry, Online © 2006–2016 John Wiley & Sons, Ltd.

This article was published in the *Encyclopedia of Analytical Chemistry* in 2016 by John Wiley & Sons, Ltd.
DOI: 10.1002/9780470027318.a5107.pub3

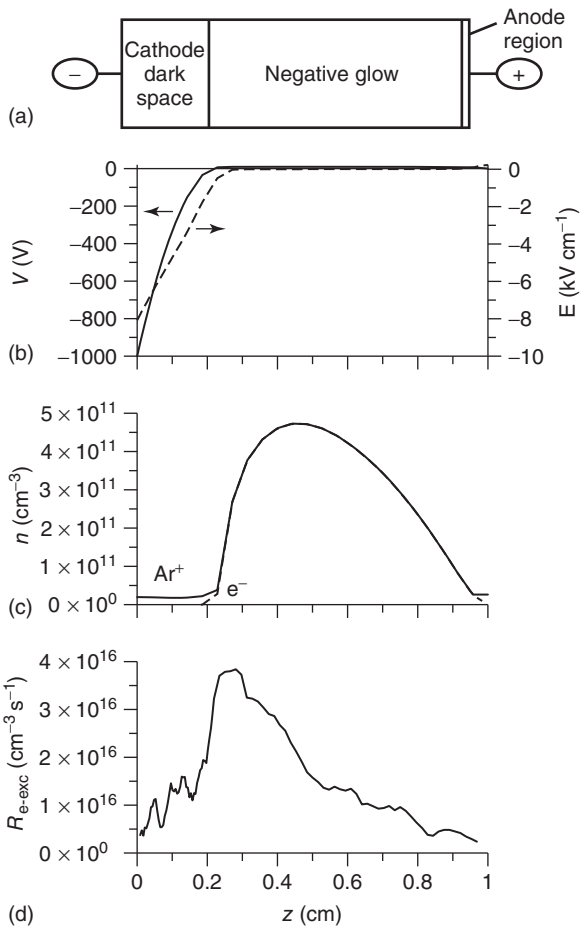

Figure 2 Schematic diagram of the different spatial regions in a glow discharge (a), the corresponding potential and electric field distributions (b), electron and Ar^+ ion number density profiles (c), and electron impact excitation rate, which gives an idea about the luminosity (d), as obtained from numerical modeling at 1000 V, 75 Pa (or 0.56 Torr), and 3 mA.

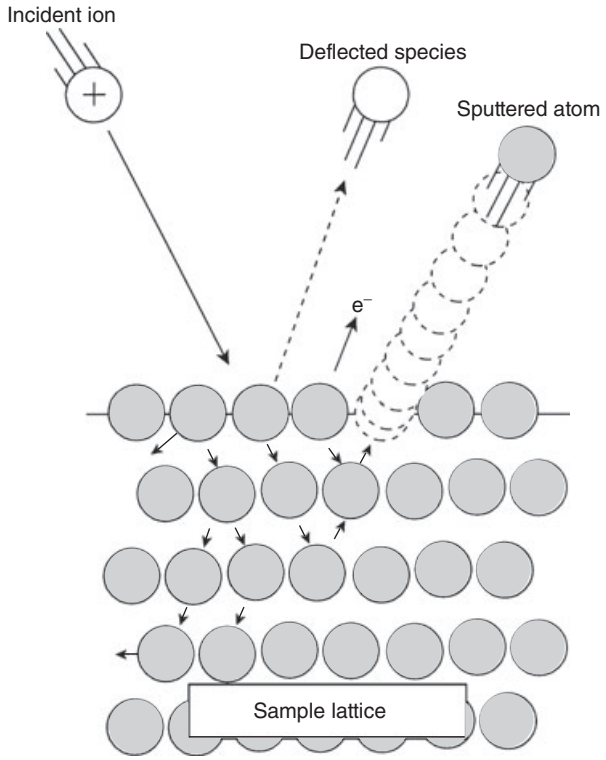

Figure 3 Illustration of cathodic sputtering process.

where W is the measured weight loss of the sample in grams, M the atomic weight of the sample, i^+ the ion current in amperes, and t the sputtering time in seconds. The ion current is related to the total current, i, by Equation (2):

$$i^+ = \frac{i}{1+\gamma} \tag{2}$$

where γ is the number of secondary electrons released, on average, by a single ion.

Much of the previous research involving sputtering has used secondary ion mass spectrometry (SIMS). Typically, ion beams generated from these types of sources are more tightly focused and of much higher energy than in GDs. This is important to note as there are a number of characteristics that affect the sputter yield for a particular system including the nature of the target, the nature of the incident species, the energy of the incident ions, and the angle of the incident ion beam. An empirical formula that is widely used for sputter yield calculations, and which describes the influence of incident ion energy and nature of incident species and target, is the Matsunami formula.[14]

2.1.2 *Excitation/Ionization Processes*

Although the atomization or sputtering process creates species essential for atomic absorption and fluorescence spectroscopies, it does not supply the excited species and ions needed for atomic emission and mass spectrometric analyses. These excitation/ionization processes occur in the collision-rich environment of the negative glow. Collisions that occur within this region not only provide analytically useful species but also are integral in maintaining the stability of the plasma. Figure 4 illustrates the three principal types of collisions that occur within the negative glow for the sputtered atoms, involving electrons, excited atoms, and ions. Excitation is dominated by electron impact (similar to Figure 4a), while ionization is governed by electron impact ionization, Penning ionization, and asymmetric charge transfer (Figure 4). In many cases, especially at low pressure

Encyclopedia of Analytical Chemistry, Online © 2006–2016 John Wiley & Sons, Ltd.

This article was published in the *Encyclopedia of Analytical Chemistry* in 2016 by John Wiley & Sons, Ltd.
DOI: 10.1002/9780470027318.a5107.pub3

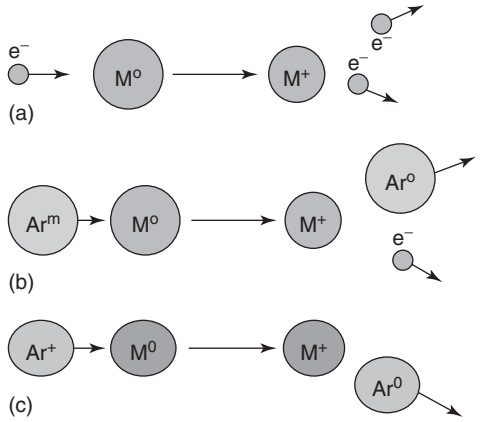

Figure 4 Illustration of the three major ionization pathways for sputtered atoms available in the GD plasma: (a) electron ionization, (b) Penning ionization, and (c) asymmetric charge transfer.

Table 2 Metastable spectroscopic notations, energies, and first ionization potentials for common discharge support gases

GD support gas	Spectroscopic notation	Metastable energy (eV)	First ionization potential (eV)
Helium (He)	2^1 S	20.6	24.5
	2^3 S	19.8	
Neon (Ne)	^{1}P0	16.7	21.6
		16.6	
Argon (Ar)	^{3}P0	11.7	15.8
		11.5	
Krypton (Kr)	^{3}P0	10.5	14.0
		9.9	
Xenon (Xe)	^{3}P0	9.4	12.1
	^{3}P2	8.3	

and voltage, Penning ionization accounts for the majority of ionization of the sputtered atoms.[7,15,16]

Electron impact ionization involves collision of an energetic electron with a gas-phase atom. Although it is of minor importance for the sputtered atoms,[15,16] it is the dominant ionization mechanism in the plasma, more specifically for the discharge gas atoms. If the electron is of sufficient energy, it can interact with an electron in the valence shell of the atom, transfer enough energy to eject the electron from the atom's electron cloud, and form an ion and a secondary electron.[17,18] There is only a small probability that such a collision will result in ionization, as defined by the ionization cross-section, which is a function of the electron energy.[19] This can be explained using classical collision theory. At the threshold, only the complete transfer of energy will result in ionization. With increase in energy of the electrons, collisions with only partial transfer of energy will result in ionization and the cross-section will increase. At high electron energies, the time and wavefunction overlap is too short for ionization to occur, and the cross-section begins to decrease.[6,19] The average energy of electrons found within the GD is not adequate enough to ionize most elements or the discharge gas.[5,20,21] However, a small percentage of electrons still has sufficient energy to ionize all elements. Chapman[5] has performed calculations, based on a Maxwell–Boltzmann distribution of electrons (which is an approximation of the real electron energy distribution, but still reasonable), to determine the percentage of electrons with energies above 15.76 eV, the first ionization potential of argon, the most common discharge gas. At an average energy of 2 eV, 0.13% of the electrons present are of sufficient energy to ionize argon. At an average electron energy of 4 eV, the percentage increases to 5.1%. A more thorough presentation of these calculations is given by Chapman.[5]

Penning ionization, named after Penning[22,23] who discovered the effect in 1925, involves the transfer of potential energy from a metastable discharge gas atom to another atom or molecule. If the first ionization potential of an atom or molecule is lower than the energy of the metastable atom, ionization will occur when they collide. Ionization cross-sections for most elements are similar for the Penning process, resulting in relatively uniform ionization efficiencies. Metastable states are reached either through the activation of a discharge gas atom to an excited state (typically by electron impact) from which radiative decay is forbidden or by the radiative recombination of discharge gas ions with thermal electrons. For argon, the most common discharge gas, the metastable levels are the $^3P_2$ and $^3P_0$ states with energy levels of 11.55 and 11.72 eV, respectively. Table 2 lists the metastable levels and energies of the discharge gases most commonly used to support GD plasmas. Metastable species are relatively long lived, existing for milliseconds under normal plasma conditions.[24] Their longevity within the plasma, along with a relatively large ionization cross-section and energy sufficient to ionize most elements, makes this process a major contributor to ion production. Investigations of ionization processes in steady-state DC-powered discharges have indicated that 40–80% of ionization occurring within these plasmas can be attributed to the Penning ionization process.[15,16,25,26] Penning ionization also affords the unique advantage of discriminating against the ionization of discharge contaminants whose ionization potentials are greater than the metastable energy of the discharge gas atoms.

The third important ionization mechanism for the sputtered atoms is asymmetric (or nonresonant) charge transfer with Ar^+ ions. Note that resonant charge exchange involves transfer of charge from one ion to an atom of the same species, whereas nonresonant charge

Encyclopedia of Analytical Chemistry, Online © 2006–2016 John Wiley & Sons, Ltd.

This article was published in the *Encyclopedia of Analytical Chemistry* in 2016 by John Wiley & Sons, Ltd.
DOI: 10.1002/9780470027318.a5107.pub3

exchange involves the transfer of charge from an ion to an atom of a different species. The first process is important in the GD as energy loss mechanism for the Ar^+ ions on their way toward the cathode, and at the same time as production process for fast Ar atoms, which can then also contribute to sputtering at the cathode.[27] The second process, on the other hand, results in the formation of ions of the sputtered material. However, it occurs only if there is sufficient overlap between the (excited) energy levels of the initial ion and the created ion. Hence, it is a more selective process than Penning ionization and electron impact ionization. Therefore, variations in relative sensitivity factors (RSFs) in GDMS are attributed to the occurrence or absence of asymmetric charge transfer as ionization mechanism for the sputtered atoms.[28,29] Because of this important role, recently, efforts were made to quantitatively determine the rate coefficient of asymmetric charge transfer between Ar^+ ions and Fe or Ni atoms, by means of the combination of plasma diagnostics and a kinetic model for the afterglow plasma.[30,31]

There are a number of other processes that play minor roles in ionization within the GD plasma. These processes involve fast Ar^+ ion and fast Ar atom impact ionization or associative ionization. Fast Ar^+ ion and Ar atom impact ionization are only important near the cathode, where the Ar^+ ions and Ar atoms have gained enough energy from the electric field for giving rise to ionization. Integrated over the entire discharge region, they account only for a few percent of the total ionization of Ar gas atoms, but this minor contribution can still be important for sustaining the discharge.[16,32] Associative ionization involves the combination of two metastable species, or the combination of a higher excited species with a gas-phase atom (i.e. the so-called Hornbeck–Molnar associative ionization), to form a molecular ion with the liberation of a secondary electron. This process contributes only marginally to ionization within the plasma, but it is the principal mechanism by which interfering metal argide ions are formed.[5]

2.2 Radiofrequency-Powered Glow Discharge Operation

Traditionally, most GD devices have used a steady-state DC-powered source. However, about two decades ago, the utility of radiofrequency (RF)-powered discharges as sources for atomic spectroscopies and mass spectrometry has been investigated.[33,34] A major advantage offered by the RF-powered plasma is the ability to directly analyze nonconducting samples such as ceramics and glasses.[35] In the past, these types of samples were typically powdered, mixed with a conductive matrix, and pressed into a pin or disk to allow analysis by the DC GD.[36–38] Utilization of an RF plasma allows the sputtering and subsequent analysis of these sample types without this added sample preparation step.

Current cannot propagate through an insulating material; therefore, when subjected to an applied DC potential, an insulator behaves in a manner similar to that of a capacitor and begins to accumulate charge. With the application of a negative voltage, the surface potential of the insulating material decays to a more positive potential with time. This decay can be attributed to charge neutralization at the cathode surface. The DC discharge will sustain itself until its threshold voltage is reached and the plasma is extinguished. Application of a high-frequency potential to a conductive material adjacent to the insulator will allow positive charges that accumulate at the nonconductor surface to be neutralized by electrons during the positively biased portion of the cycle. Therefore, application of a high-frequency potential will allow a negative potential to be maintained on the nonconductor's surface.

Figure 5 illustrates the phenomenon known as *cathode self-biasing* that allows the discharge to be maintained for long periods of time.[5] Self-biasing is based on the mobility difference between ions and electrons. As a negative potential is initially applied, the surface gets charged quickly, reaches a maximum, and begins to decay owing to the bombardment of positive ions (Figure 5b). When the potential is switched, electrons are accelerated and bombard the surface much like the positive ions during the negatively biased portion of the cycle. The electrons, however, have a greater mobility than the more massive positive ions; therefore, the surface potential decays more quickly. After a number of cycles, the waveform will reach a steady negative DC offset. In typical GDs used for analytical applications, where a large difference in size exists between powered RF electrode (i.e. sample) and grounded electrode (i.e. cell housing), this DC offset potential is approximately one half of the applied peak-to-peak voltage and sustains the sputtering ion current.[39,40] Indeed, because of this negative DC offset, the sample will be continuously bombarded by positive ions, but this charging will be compensated by the bombardment of a high flux of electrons during a small portion of the RF cycle.[39] Operation in this mode has proven useful for the analysis of materials such as nonconducting alloys, oxide powders, and glass samples.[41]

2.3 Pulsed Operation of the Glow Discharge

The GD plasma can be operated in a modulated power mode as well as in the steady-state mode described previously. Pulsed power operation offers some distinct analytical advantages that make it attractive to the analyst.[42–49] Steady-state discharges are power limited

Encyclopedia of Analytical Chemistry, Online © 2006–2016 John Wiley & Sons, Ltd.

This article was published in the *Encyclopedia of Analytical Chemistry* in 2016 by John Wiley & Sons, Ltd.
DOI: 10.1002/9780470027318.a5107.pub3

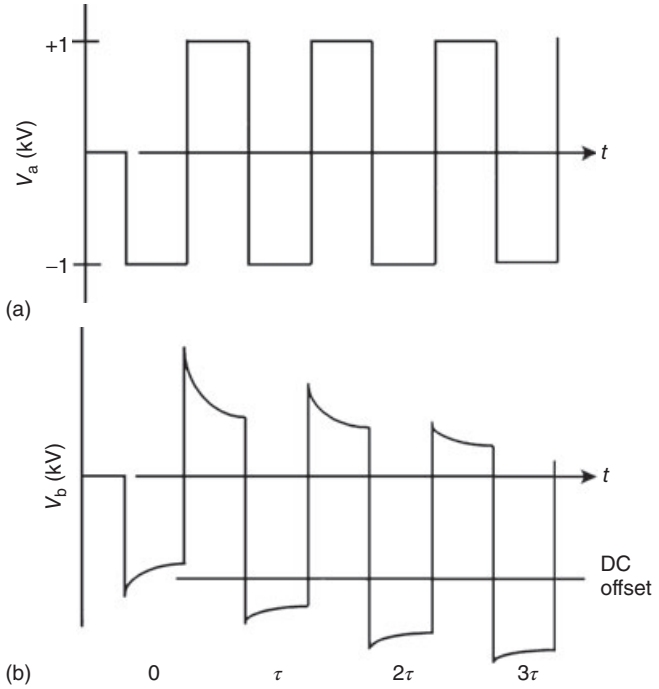

Figure 5 Electrode response to an applied square wave potential: (a) V_a, applied voltage and (b) V_b, response voltage. (Reproduced with permission from Ref. 5. © John Wiley & Sons, Ltd., 1980.)

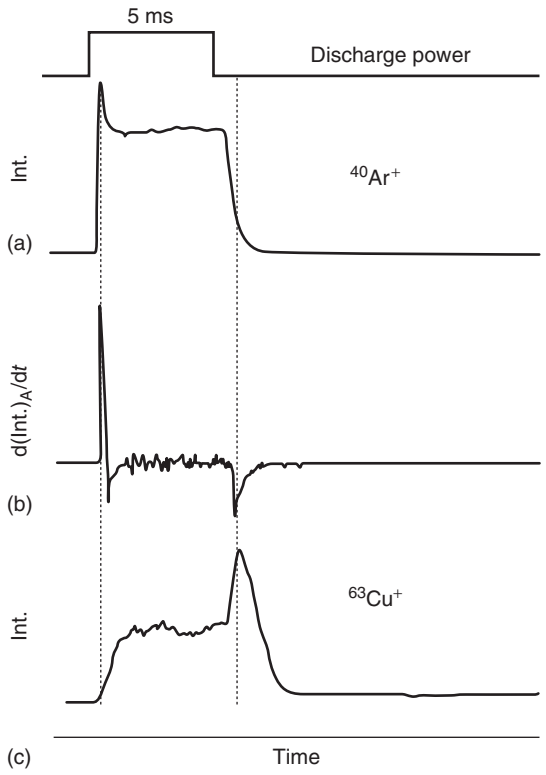

Figure 6 Temporal ion signal profiles: (a) discharge gas ions, $^{40}Ar^+$; (b) the first derivative of the $^{40}Ar^+$ profile; and (c) sputtered analyte ions, $^{63}Cu^+$. (Reprinted with permission from F. L. King, C. Pan, Time-resolved Studies of Ionized Sputtered Atoms in Pulsed Radio-frequency Powered Glow-discharge Mass Spectrometry, *Anal. Chem.*, **65**, 3187–3193., (1993) © (1993) American Chemical Society.)

because increased power application results in resistive heating of the cathode, eventually jeopardizing sample integrity.[50] Modulation of the applied discharge power permits operation at higher instantaneous power while keeping the average power at an acceptable level. This operation mode serves to increase the sputter yield by increasing the average energy and/or the number of incident ions, leading to higher signal intensities and hence better analytical sensitivities,[51] while allowing the sample to cool during the off portion of the discharge cycle. Modulated operation also provides temporal segregation of discharge processes (see below).

Modulated GD operation relies on a microsecond to millisecond square wave power pulse, with a duty cycle of 10–50%. These parameters allow sufficient time for cooling and for the removal of species from one pulsed event before the next one is initiated. Figure 6 depicts a typical pulse sequence showing both discharge gas (Ar) and analyte ion signal profiles. It is apparent that signal behaviors for discharge gas and analyte species differ significantly. Upon power initiation, the discharge gas ion signal exhibits a sharp rise in intensity to a maximum[44,52] (Figure 6a). This 'prepeak' results from the electrical breakdown of the discharge gas species upon power application. The short delay occurs because the acceleration of electrons and subsequent electron ionization of the discharge gas are not instantaneous processes. In contrast, the analyte ion profile behaves differently (Figure 6c). A much longer delay occurs before a more gradual signal increase is observed. This delay arises because sample atoms must first be sputtered from the cathode surface and diffuse into the negative glow region before they can undergo ionization. The temporal correlation between the observation of discharge gas ions and the appearance of analyte signal can be seen in Figure 6. Both signals reach equilibrium conditions about half way through the applied power pulse in the 'plateau' region. During this time regime, the plasma most closely approximates the behavior of a steady-state plasma.

Upon applied power termination, the two ion profiles again show markedly different behavior. The discharge gas ion profile decreases quickly ($\approx$500 μs) upon power termination. Previous studies have explained this signal decay as the rapid recombination of discharge gas ions with thermal electrons to form metastable discharge gas

Encyclopedia of Analytical Chemistry, Online © 2006–2016 John Wiley & Sons, Ltd.

This article was published in the *Encyclopedia of Analytical Chemistry* in 2016 by John Wiley & Sons, Ltd.
DOI: 10.1002/9780470027318.a5107.pub3

atoms.[53,54] The analyte ion profile quickly increases during the 'afterpeak' region, reaching a maximum shortly after pulse power termination. This signal then decreases gradually to the baseline. Figure 6(b) represents the first derivative of the discharge gas ion signal profile. The maximum and minima observed in this portion of Figure 6 represent the temporal location of the respective maximum signal intensity increases and decreases for the discharge gas signal. Interestingly, the maximum decrease in the discharge gas ion signal corresponds to the afterpeak maximum for the analyte species.[50] This correlation supports the theory that at power termination electrons are collisionally cooled and recombined with argon ions, forming metastable species. This theory is further supported by measurements of the Ar metastable atom density, which exhibits a maximum far away from the cathode, within the first 100 μs after pulse termination.[55]

This increase in metastable argon atoms increases the probability of ionization via the Penning process, thus providing enhancements in the analyte ion signal. Nowadays, this explanation is generally accepted.[56–58] However, it is not completely clear which recombination processes are responsible for the formation of metastable atoms.[59,60] Indeed, on the basis of calculated electron and Ar^+ ion densities and recombination rate coefficients available from literature, recombination of Ar^+ ions and electrons seems not to be efficient enough. It is suggested[60] that dissociative recombination of Ar_2^+ ions with electrons might be the most efficient recombination process in the afterglow.

Temporally gated separation and detection of species found in these distinct plasma regions increase the utility of the GD devices.[50,61] The most analytically useful region is the afterpeak. Data acquired within this time regime offer two advantageous characteristics. As illustrated in Figure 6(c), the signal intensity for the analyte species increases substantially, thus potentially enhancing the sensitivity for analyte species in this region. The other advantage arises from the suppression of electron-ionized interfering species.[43,44] The first ionization energies of the discharge gas and molecular contaminants (e.g. H_2O, N_2, and O_2) are too high to allow ionization through the Penning process. Upon power termination, species that are ionized via electron impact are no longer excited. Thus, if the acquisition gate is moved far enough into the afterpeak, contributions from these species will be minimized.

Temporally gated detection of the emission lines can also give important insight in the excitation and recombination processes of analyte and fill gases. It was found that in a microsecond-pulsed GD, lines originating from low-energy levels have smaller afterpeaks than lines arising from high-energy levels, suggesting that in a microsecond-pulsed GD, highly excited argon and copper atoms are probably generated through electron-ion three-body recombination, in contrast to millisecond-pulsed GD, where dissociative recombination was reported as an important mechanism.[62] Furthermore, side-on measurements of the emitted radiation of a pulsed RF-GD revealed that the spatial distribution of Ar and Cu emission differs from each other: the Ar atom emission extends longer in the plasma than the Cu atom emission, and the ions have their maximum emission close to the anode. This suggests that it is possible to detect ionic emission at distances far away from the negative glow, in regions where usually the sampler cone is placed in GDMS.[63]

Finally, some other distinct advantages of pulsed discharges are the low overall sputter rates (in combination with high transient sputter rates and hence high signal intensities) opening possibilities in the field of thin film analysis[64,65] (in fact, a wide dynamic range of layers, from several nanometers to tens of micrometers thick, can be analyzed[66]), as well as the ability to obtain structural, molecular, and elemental information of samples.[67–69] Indeed, depending on the extent of interaction with the plasma, the samples may undergo soft chemical ionization, yielding molecular ions or they may be completely atomized and ionized, yielding elemental information.

2.4 Applications

In the early 1970s, as GD instrumentation and techniques were being transitioned from research applications to routine sample analysis, spark source techniques reigned as the analytical tool of choice for trace analysis of solids. Spark source spectrometry was limited, however, by its expense, complexity, and unreliability. These disadvantages associated with spark source spectrometry facilitated the acceptance of the GD for the analysis of solid samples.

2.4.1 Bulk Analysis

Historically, GD mass spectrometry and optical spectroscopies have proven most valuable for the analysis of bulk conductive solid samples. As explained earlier, GD methods provide a representative gas-phase analyte population directly from samples in the solid form, thus significantly simplifying sample preparation. GD techniques can also be used for the analysis of nonconducting samples such as glasses, polymers, and ceramics.[70–72] The first analyses of nonconducting materials involved mixing a powdered sample with an easily sputtered, conducting matrix, such as high purity copper or silver powder.[73–76] The mixture was pressed into a sample cathode using a die and hydraulic press system.

Encyclopedia of Analytical Chemistry, Online © 2006–2016 John Wiley & Sons, Ltd.

This article was published in the *Encyclopedia of Analytical Chemistry* in 2016 by John Wiley & Sons, Ltd.
DOI: 10.1002/9780470027318.a5107.pub3

Unfortunately, this complicated sample preparation, especially for samples that were not in powdered form. Homogeneity of the mixed sample also became a matter of concern for the analyst. Two other methods for the analysis of nonconducting samples have also been used. These methods do not require sample mixing but rather use an RF-powered or a secondary cathode GD source to directly sample solid nonconducting materials. Section 2.2 describes plasmas powered by RF sources. Secondary, or sacrificial, cathode GD systems utilize a monoisotopic conductive mask (e.g. Ta, Pt) that is placed on top of the sample to be analyzed. A potential is applied to the mask, which thus assumes the role of the cathode. As material is sputtered from the mask, a large portion of it is redeposited on the surface of both the secondary cathode and the nonconducting sample. At this point, the layer of cathode material deposited onto the sample becomes conductive and thus assumes the applied potential and attracts impinging ions. As ions impinge on the cathodic layer, they ablate both the cathodic material and the underlying nonconductor, introducing both species into the gas phase for subsequent analysis. It is clear that the mask material must not contain species that are of interest because this will contaminate the sample and preclude accurate measurements. A number of references are available describing in detail the use of secondary cathodes.[77–79]

2.4.2 *Surface and Depth-Profiling Analysis*

A few decades ago, surface and depth-profiling analysis by GD spectrometry has aroused great interest in the analytical community. In a sense, GD is always a surface analysis technique, acting as an atomic mill to erode the sample surface via the sputtering process. Atoms sputtered from the surface are subsequently measured using either optical or mass spectrometric techniques. GD sputtering consumes relatively large quantities of the sample in a relatively short time period (up to mg min^{-1}). This makes analysis of thick layers ($>10\,\mu m$) possible, but on the other hand, thin films of less than 10 nm thickness can be analyzed as well, by proper choice of plasma conditions.[80–82] Figure 7 is a graphical illustration of a typical spectral intensity–time profile of a multilayer coating prepared by chemical vapor deposition of carbon steel. The outer layer consists of vanadium carbide and the inner layer chromium carbide. It is obvious from Figure 7 that signal responses do not follow an ideal square wave pattern for appearance and disappearance. Clearly, the metal sample layer is not completely eroded at a well-defined time but is scattered across a diffuse region that is gradually removed. This signal tailing can be a manifestation of nonflat crater profiles,[84,85] or it can be due to the redeposition that

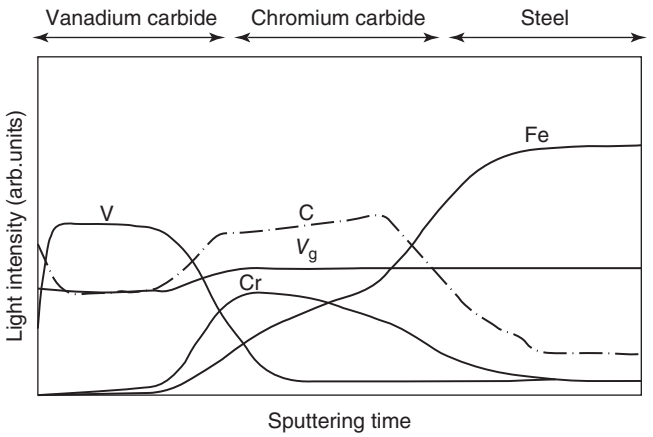

Figure 7 Qualitative analysis of multilayer coating. V_g, voltage. (Reproduced with permission from Ref. 83. © Springer, 1993.)

occurs from the plasma. It has been estimated[84–86] that up to 67% of the sputtered atom population is returned to the surface by collisions with argon atoms, to be resputtered before eventually escaping permanently from the surface. By calibrating erosion rates using standard layered samples, the thickness of layers can be determined by analyzing the signal–time profiles, allowing the full characterization of sample layers. Nowadays, GDs, mostly in the Grimm-type configuration, are widely used for depth-profiling and thin-film analysis of various materials, including ultrathin (approximately nanometer sizes) multilayers.[80–83,87–95] The application of mathematical tools, such as deconvolution algorithms and a depth-profiling model, pulsed sources, and surface plasma cleaning procedures, can greatly improve the GD-OES depth resolution.[90]

Recently, RF-GD-TOF-MS (in pulsed and continuous mode) was optimized for molecular depth profiling and for the identification of organic polymers.[91] Especially the pulsed mode was found to offer a great analytical potential to characterize such organic coatings. Moreover, some formed polyatomic ions appeared to be useful to identify the different polymer layers, so that layers with similar elemental composition but different polymer structure could also be identified. From a comparison of the results of RF-GD-TOF-MS with those obtained with TOF-SIMS, it appears that the analytical performance of both techniques was comparable, although with a poorer depth resolution for GD-TOF-MS, but the analysis time was much shorter, the cost was reduced, and the restrictions imposed by the need of ultrahigh vacuum conditions of SIMS could be avoided.[92] Hence, RF-GD-TOF-MS can be a valuable alternative to SIMS, in those cases where lateral resolution is not required.

Encyclopedia of Analytical Chemistry, Online © 2006–2016 John Wiley & Sons, Ltd.

This article was published in the *Encyclopedia of Analytical Chemistry* in 2016 by John Wiley & Sons, Ltd.
DOI: 10.1002/9780470027318.a5107.pub3

A new development of the past few years is the improvement of surface elemental imaging by GD-OES.[96−99] In this way, lateral information from the sputtered sample can be obtained, with a depth resolution maintained below 10 nm.[97] GD-OES elemental mapping thus offers high-throughput determination of the 3D surface elemental composition of large areas of samples. Possible applications range from the characterization of the homogeneity of reference materials to quantification and identification of proteins in mixtures separated by 2D gel electrophoresis.[99]

2.4.3 Analysis of Solution and Gaseous Samples

In the past decades, there is increasing interest in the analysis of solutions and gaseous samples using GD techniques, even though their major advantage lies in the ability to directly analyze solid-state samples. It is important to note that aspiration of a solution directly into the GD will cause quenching of the plasma, making the removal of any solvent from the sample preferable. The simplest and most direct method of doing this is to evaporate a solution onto a conducting cathode, leaving a dried residue as the sample. A more elegant method for depositing solution samples onto a cathode involves electrodeposition. This approach also permits analytes in large sample volumes to be preconcentrated before analysis. Solutions containing samples have also been mixed with a conductive powder and dried for subsequent analysis. This approach is similar to that used for the analysis of nonconductive powders.

Direct analysis of solution samples by GD techniques has been performed for specialized applications. Strange and Marcus[100] have used a particle injection system to introduce a solution sample into the GD. Steiner et al.[67] have also utilized a pulsed plasma TOF system to obtain concurrent elemental and molecular information for high-vapor pressure liquid samples.

The increasing interest in novel applications for liquids and gaseous analysis is catalyzed by the development of new types of GD plasma sources, often working at atmospheric pressure and/or with reduced dimensions. With respect to liquids analysis, the so-called electrolyte cathode atmospheric glow discharge (ELCAD) was developed in 1992 by Cserfalvi and Mezei.[101] More detailed information of this system, including its main operating parameters, mechanisms, and analytical performance, can be found in Ref.[102] Hieftje and coworkers have adopted (and modified) this concept of the ELCAD, among others, for exploring the analysis of complex samples.[103,104] Furthermore, a new design of a solution-cathode GD, with a smaller volume and a corresponding increase in power density compared to the ELCAD-like designs, was also developed,[105] as well as another type of small-scale plasma, the so-called annual GD,[106] where aerosol is introduced in the plasma through the cathode, and atomic emission is observed in the near-cathode region. Several other authors also applied the ELCAD or developed different types of source designs for liquid analysis, e.g., based on a liquid-film dielectric barrier discharge (DBD)[107] or a dielectric capillary barrier discharge.[108,109] Marcus et al.[110] developed the liquid sampling-atmospheric pressure glow discharge (LS-APGD) and the particle beam (PB) sample introduction system of liquid samples, to be used in combination with hollow cathode optical emission spectrometry (PB/HC-OES) and with GDMS (PB/GDMS).[111] More recently, they also converted a commercially available gas chromatography mass spectrometer (GC/MS) into a liquid chromatography particle beam (LC-PB) GDMS system.[112]

For gaseous analysis, several new source designs were developed as well.[113−118] Hieftje and coworkers developed a novel versatile DC APGD in He, interfaced with a TOF-MS system.[113] When this detection system is coupled with hydride generation, the analytical performance of the hydride generation APGD is comparable to that of an ICP source. Detection down to 10 ppt could be realized. A spectroscopic characterization of a new DC APGD in He was presented by Broekaert and coworkers.[114] Newman and Mason[115] introduced organic vapors into the flowing afterglow of a lower power DC GD coupled to a quadrupole mass spectrometer, Fliegel et al.[116] evaluated the use of a pulsed GD-TOF-MS system as a detector for gas chromatography analysis, and Franzke and coworkers[117] presented a low-cost microhollow cathode discharge (MHCD) for gaseous atomic emission spectrometry and showed that this microplasma chip might be suitable for lab-on-a-chip applications. A further improvement, where the plasma is formed inside a microfabricated multilayer structure with a dielectric barrier, prevents deterioration of the electrodes and eliminates contamination of the gaseous analyte with electrode material, and thus allows long-term operation of the system over several days.[118]

Finally, an emerging field for the analysis of either gaseous or solid compounds is the so-called ambient desorption/ionization mass spectrometry (ADI-MS). Sample pretreatment and separation steps are eliminated here by directly desorbing and ionizing analytes from a sample surface, for analysis by mass spectrometry.[119] One of the problems ADI-MS is facing is that it suffers from matrix effects. Therefore, Shelley and Hieftje[120] investigated ionization-related matrix effects in three plasma-based ADI-MS sources, i.e. the flowing atmospheric pressure afterglow (FAPA), direct analysis in real time (DART), and the low-temperature plasma (LTP) probe, which is based on a DBD design. The FAPA was

Encyclopedia of Analytical Chemistry, Online © 2006–2016 John Wiley & Sons, Ltd.

This article was published in the *Encyclopedia of Analytical Chemistry* in 2016 by John Wiley & Sons, Ltd.
DOI: 10.1002/9780470027318.a5107.pub3

found to be the least susceptible to ionization matrix effects in every case, but when the proton affinity of the matrix species was lower than that of the analyte, no matrix effects were observed at all for DART, whereas an effect persisted for both FAPA and LTP. Moreover, also Kratzer et al.[121] compared three plasma-based ambient pressure sources, i.e. a laboratory built DBD, an RF-driven APGD, as well as a commercial DART source, for ADI-MS of acetaminophen.

3 SPECTROCHEMICAL METHODS OF ANALYSIS

The goal of an analytical chemist is often to identify a particular chemical species or to quantify the amount of that species in a sample. In a spectrochemical analysis, the chemist uses the intensity of radiation emitted, absorbed, or scattered by a particular species versus a quantity related to photon energy, such as wavelength or frequency, to make such measurements.[122]

In this section, the basic requirements necessary to obtain a spectrochemical analysis are reviewed, along with three spectrochemical methods that are used to effect the measurement: AAS, AES, and luminescence spectroscopy. Although there are many variations of each of these methods, we review only the classical approaches and the variations that have been used with GD devices. Table 3 summarizes the quantity measured and gives examples associated with each measurement technique.[122]

Table 3 Classification of spectrochemical methods[123]

Class	Quantity measured	Examples
Emission	Radiant power of emission	Flame emission, DC arc emission, spark emission, inductively coupled plasma and direct current plasma emission, GD emission
Absorption	Absorbance or ratio of radiant power transmitted to that incident, $A = \log(\Phi/\Phi_0)$	UV/visible molecular absorption, IR absorption, atomic absorption
Luminescence	Radiant power of luminescence, Φ_L	Molecular fluorescence and phosphorescence, atomic fluorescence, chemilumines-cence

UV, ultraviolet; IR, infrared.
Reproduced with permission from Ref. 123. © Prentice Hall, 1988.

3.1 Basic Requirements Necessary to Obtain Optical Information

For thousands of years, scientists have been performing qualitative analyses based on color, smell, taste, size, and shape. Although first-year college chemistry students are still taught to use their senses to help identify substances in qualitative laboratory, for the rest of us these less-precise approaches have been replaced with chemical and instrumental methods that can measure not only pure materials but also trace components in complex mixtures. However, most materials do not give this information spontaneously. Instead, to obtain chemical information about a sample, it is necessary to perturb the sample through the application of energy in the form of heat, radiation, electrical energy, particles, or a chemical reaction.[122] The application of this energy often causes electrons in analytes to be excited from their lowest energy or ground state to a higher energy or excited state. Several spectroscopic phenomena depend on these transitions between electronic energy states.[122] Information can be obtained by measuring the electromagnetic radiation emitted as the electron returns to its ground state from an excited state (emission), by measuring the amount of radiation absorbed in the excitation process (absorption), or by measuring the changes in the optical properties of the electromagnetic radiation that occur when it interacts with the analyte (e.g. ionization or photochemical reactions). Qualitative information is extracted by observing a particular element-specific transition, whereas quantitative information is obtained by quantifying the amount of radiation emitted or absorbed in that transition. Figure 8 is an illustration used by Ingle and Crouch[122] to depict the many processes involved in converting concentration information into a number – the analytical chemist's goal in making a measurement. A sample introduction system presents the sample to the encoding system, which converts the concentrations c_1, c_2, and c_3 into optical signals O_1, O_2, and O_3. The GD is slightly unusual (compared with other atomic sources such as the flame or the inductively coupled plasma) because it serves as both the sample introduction system (through sputter atomization) and the spectrochemical encoder. The information selection system (often a monochromator) selects the desired optical signal O_1 for presentation to the radiation transducer or photodetector. This device converts the optical signal into an electrical signal that is processed and read out as a number. All spectrochemical techniques that operate in the ultraviolet (UV)/visible and infrared (IR) regions of the spectrum employ similar instrumentation[122]; the only differences lie in

Encyclopedia of Analytical Chemistry, Online © 2006–2016 John Wiley & Sons, Ltd.

This article was published in the *Encyclopedia of Analytical Chemistry* in 2016 by John Wiley & Sons, Ltd.
DOI: 10.1002/9780470027318.a5107.pub3

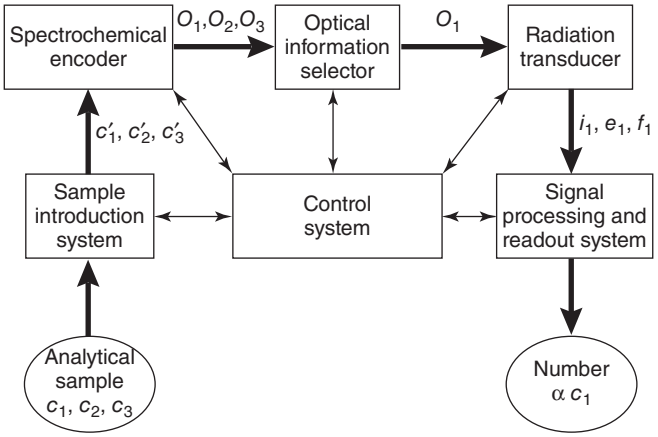

Figure 8 Spectrochemical measurement process. (Reproduced with permission from Ref. 122. © Prentice Hall, 1988.)

the arrangement and type of sample introduction system, encoding systems, and information selection system.

3.1.1 Spectrometers

The optical information selector in Figure 8 sorts the desired optical signal from the many signals produced in the encoding process. Although it is possible to discriminate against background signals on the basis of time and position, most often discrimination is based on optical frequency (wavelength). The most widely used wavelength selection system is the monochromator, although there are a variety of other systems, including polychromators and spectrographs, and nondispersive systems such as the Fabry–Perot, Michelson, Mach–Zender, and Sagnac interferometers. Our discussion is limited to monochromators; for a thorough discussion of other types of wavelength selection systems, the reader is directed elsewhere.[122]

Monochromators isolate one wavelength from the countless number of wavelengths found in polychromatic sources. A monochromator consists of two principal components: a dispersive element and an image transfer system. Light is transferred from an entrance slit to an exit slit by a series of mirrors and lenses; along the way it is dispersed into its various wavelengths by a grating (or sometimes a prism). To change wavelengths, one rotates the dispersive element, which results in different wavelength bands being brought through the exit slit in succession. One can easily calculate the angular dispersion (D_a) (i.e. the angular separation [$d\beta$] corresponding to the wavelength separation [$d\lambda$]) of a grating by knowing the angle of incidence, the angle of diffraction, the order of diffraction, and the groove spacing of the grating. For practical purposes, however, it is more important to calculate the linear dispersion, $D_l = dx/d\lambda$ (a value that defines how far apart in distance two wavelengths are separated in the focal plane), or the reciprocal linear dispersion, R_d (the number of wavelength intervals contained in each interval distance along the focal plane).

A monochromator's resolution is closely related to its dispersion in that dispersion determines how far apart two wavelengths are separated linearly while an instrument's resolution determines whether the two wavelengths can be distinguished. In many cases, the resolutions determined by the monochromator's spectral bandpass, s, defined as the half-width of the wavelength distribution passed by the exit slit. If the slit width is large enough to ignore aberrations and diffraction, a scan of two closely spaced monochromatic lines of peak wavelengths λ_1 and λ_2 will be just separated (baseline resolution) if $\lambda_2 - \lambda_1 = 2s$. Therefore, the slit-width-limited resolution $\Delta\lambda_s$ is given by Equation (3):

$$\Delta\lambda_s = 2R_d W \tag{3}$$

where W is the slit width.[122] By adjusting the monochromator so that $\Delta\lambda_0 = \Delta\lambda_1$ and $W = \Delta\lambda/R_d$, the image of λ_1 will be completely passed, while that of λ_2 will be at one side of the exit slit.[122]

3.1.2 Detectors

Two detectors are most often used in atomic spectroscopy: photomultipliers (the most common) and multichannel detectors. A photomultiplier is a more sophisticated version of a vacuum phototube. A cascade of electron collisions with dynodes of increasing potential and the subsequent ejection of electrons from each dynode's surface leads to the formation of an electrical current proportional to the number of photons striking the detector. The process begins with a photon striking a cathode made of a photoemissive material (e.g. alkali metal oxides, AgOCs, CS_3Sb). If the energy of the photon is above some threshold value, an electron is ejected from the cathode. Only a certain fraction of the photons with energy greater than threshold produce photoelectrons with sufficient KE to escape the photocathode. This fraction is called the *quantum efficiency* and is the ratio of the number of photoelectrons ejected to the number of incident photons. After leaving the photocathode, a photoelectron strikes the first dynode of the multiplier; this causes the subsequent ejection of two to five secondary electrons, which in turn are accelerated by an electric potential to a second dynode where they cause the release of two to five more electrons. This multiplication process continues until the electrons reach the last dynode and impinge on the anode. A modern photomultiplier tube might have 5–15 dynodes (made of

Encyclopedia of Analytical Chemistry, Online © 2006–2016 John Wiley & Sons, Ltd.

This article was published in the *Encyclopedia of Analytical Chemistry* in 2016 by John Wiley & Sons, Ltd.
DOI: 10.1002/9780470027318.a5107.pub3

a secondary emission material such as MgO or GaP) in a cascade. The result of this photomultiplication is that for each photoelectron collected by the first dynode, a large number of charges are produced at the anode, within a few nanoseconds. Photomultipliers can be operated either in analog mode, where the average current that results from the arrival of many anodic pulses is measured, or in photon counting mode, where the number of anodic pulses, and not photons, is counted per unit time.

A wide variety of photomultipliers are available with both end-on and side-on viewing for adaptation to a wide variety of monochromators. Care must be given to the wavelength range over which one is working to ensure a uniform response. Other concerns for the spectroscopist, all of which are beyond the scope of this article, include the quantum efficiency of the photomultiplier, the multiplication factor of each dynode, the operating (accelerating) voltages applied to the dynodes, and the dark current generated when a potential is applied between the anode and cathode, with no photons hitting the photocathode.

The second type of detector that is widely used in atomic spectroscopy is the multichannel detector. These devices include early photographic detectors such as photographic film or plates, as well as modern detectors such as photodiode arrays and charge-coupled and charge-injection devices. The idea behind the multichannel detector is simultaneous detection of dispersed radiation. Modern multichannel detectors usually take the form of some sort of solid-state *pn*-junction diode device packaged in integrated-circuit form with a large number (e.g. 256, 512, or 1024) of elements arranged in a linear manner. These devices often have linear dynamic ranges of two to four orders of magnitude. Limitations at the low end result from the noise associated with readout of a given dynode. Limitations at the upper end are the result of saturation; this is determined by the number of electron–hole pairs that can be created. A typical saturation charge is 1–10 pC. The reader is referred to several excellent references for a more thorough description of multichannel detectors.[123–125]

3.2 Atomic Emission Spectroscopy

AES is the simplest spectroscopic method for determining the elemental composition of a sample and is the logical starting point for a discussion on atomic spectrometry. Optical emission results from electron transitions occurring within the outer electron shells of atoms. These transitions give rise to line spectra where the wavelength of the lines relates to the energy difference of the levels according to Equation (4):

$$\Delta E = \frac{hc}{\lambda} \tag{4}$$

Spectroscopists often categorize spectral transitions according to term symbols. For a complete discussion of term symbols, the reader is referred elsewhere[126]; a brief discussion follows.

Each electronic state of an atom has five quantum numbers that define its electronic configuration. These include the principal quantum number, n; the orbital angular momentum quantum number, l; the orbital magnetic quantum number, mi; the electron spin quantum number, s; and the spin magnetic quantum number, ms. According to Ingle and Crouch,[122] for many-electron atoms, the hydrogen quantum numbers can be thought of as describing the individual electrons, but they are not 'good' quantum numbers for the entire atom. Good quantum numbers are associated with operators that commute with the total atom Hamiltonian. These include the resultant orbital angular momentum quantum number, L, produced by coupling the orbital angular momenta of each electron and the resultant spin quantum number, S. For atoms with weak spin–orbit interactions, L and S couple to produce a total angular momentum quantum number, J. A multiplet of closely spaced states with the same L and S values but different J values is called a *spectroscopic term* and is designated as $n^{2S+1}\{L\}_J$, where n is the principal quantum number for the valence electrons, $2S+1$ defines the multiplicity, and J is the total angular momentum quantum number. Of all the possible transitions between states, only a fraction of them are observed. From quantum mechanical principles, it is possible to derive selection rules that tell which transitions are allowed (i.e. those that occur with high probability and give reasonably intense lines) and which are forbidden (i.e. those that occur with low probability and give weak lines); this is beyond the scope of this article. For this discussion, it is sufficient to note that term symbols for almost all practical configurations have been tabulated[126] and tables of spectral line intensities have been assembled for nearly all the elements.[127]

In AES, the information relevant to an analysis can be found in the radiation emitted by excited analyte atoms decaying from a nonradiational activation event. The radiant power of this emission is a function of several factors, including the population density of the excited atoms, the number of photons emitted per second by each atom, the energy of each photon, and the volume of the emitting system. The reader is directed elsewhere for a more complete discussion of each of these factors.[122]

AES has the power to provide rapid, qualitative, and quantitative multielement analyses. Although a qualitative survey of the elements (i.e. a plot of the analytical signal versus wavelength) in a sample may be useful, more often the desired information is the concentration of an analyte. Unfortunately, this is almost never obtained directly as the result of an absolute

Encyclopedia of Analytical Chemistry, Online © 2006–2016 John Wiley & Sons, Ltd.

This article was published in the *Encyclopedia of Analytical Chemistry* in 2016 by John Wiley & Sons, Ltd.
DOI: 10.1002/9780470027318.a5107.pub3

measurement of an optical signal because the amplitude and elemental concentration are seldom related in a simple way. Obtaining the desired concentration from an optical measurement usually involves calibration, subtraction of blanks, comparison with standards, and other similar procedures.[122] Quantitative analysis of a single element is most easily accomplished in AES by monitoring the emission intensity as a function of the analyte's concentration under a given set of conditions (e.g. constant discharge gas pressure, voltage, and current at a given wavelength). Standards, often provided by the National Institute of Standards and Technology, provide a range of concentrations over which a calibration curve can be developed. The signal intensity of an unknown concentration is then compared with the intensity of the standards, thus providing the concentration of the analyte in question.

Although simple in principle, quantification is complicated by a number of factors, including spectral background, incomplete wavelength separation, self-absorption, peak broadening, and so on, most of which are beyond the scope of this article. When one considers these complicated issues, it is clear why it is important to control conditions precisely and use standards for the most accurate quantification.

Instrumentation used for emission spectroscopy includes an excitation source, a sample container, a wavelength selector, and a radiant power monitor. Depending on the spectrochemical method, the excitation source and sample container may be separate components or they may be combined, as is the case with the GD. Figure 9 illustrates one instrumental configuration used in our laboratory at the Oak Ridge National Laboratory for AES. A 0.5-m monochromator serves as the wavelength selector and the combination of a photomultiplier tube, preamplifier, and readout photometer comprises the radiant power monitor. Figure 9 also illustrates three common sources used with GD emission spectroscopy – a planar cathode discharge and two versions of the hollow cathode discharge.

The planar cathode discharge is thus termed because the portion of the sample exposed to the discharge is flat. It is often contrasted with the coaxial or pin-type cathode used more commonly with mass spectrometry and described elsewhere in this article. With the development of the Grimm lamp in 1968[8] and its eventual commercialization, the planar cathode discharge gained widespread use for emission spectroscopy. Although other planar cathode discharges have been developed in the past 40 years, the Grimm source still finds the

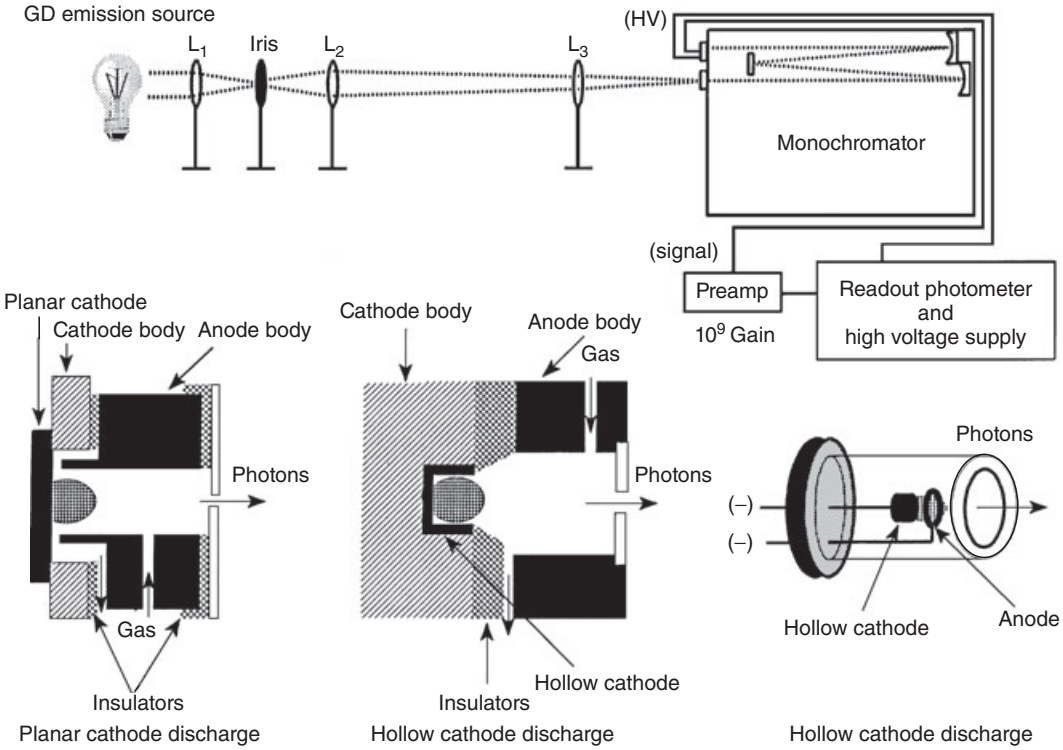

Figure 9 Schematic of an instrumental arrangement used at the Oak Ridge National Laboratory for AES. (Reprinted with permission from W. W. Harrison, C. M. Barshick, J. A. Klingler, P. H. Ratliff, Y. Mei, Glow Discharge Techniques in Analytical Chemistry, *Anal. Chem*., **62**, 943A–949A., (1990) © (1990) American Chemical Society.)

Encyclopedia of Analytical Chemistry, Online © 2006–2016 John Wiley & Sons, Ltd.

This article was published in the *Encyclopedia of Analytical Chemistry* in 2016 by John Wiley & Sons, Ltd.
DOI: 10.1002/9780470027318.a5107.pub3

greatest application today. One interesting feature of the Grimm source is that it is an obstructed discharge (i.e. the discharge is confined to the sample by the extension of the anode into the cathode dark space). Moreover, the vacuum in the anode–cathode inner space is lower than in the discharge region itself, necessitating a dual outlet pump with a larger throughput for the inner electrode space.[128] Another interesting feature of the Grimm source is that the cathode is located outside of the source itself; this provides for easy sample interchange and means that the Grimm source is particularly amenable to the analysis of any flat conducting surface that can be brought up to the source opening, such as metal sheets or disks. Typical operating conditions for the Grimm source are 500–1000 V, 25–100 mA, and 1–5 Torr. The relatively high power produced by the source (12.5–100 W) means that the cathode is often water-cooled; this usually is not a problem in emission spectroscopy, but makes interfacing the Grimm source with a mass spectrometer (with its high vacuum requirements) more difficult.

Planar cathode discharges have been interfaced to a variety of commercial emission instruments.[10] Grimm-type sources find their greatest use in trace elemental analysis of solids and in-depth profiling of layered metal samples.[128] Detection limits by emission spectroscopy are of the order of 0.1 ppm.[10] Precision of the order of 0.5–5% has been obtained for concentrations in the 0.01–10 mg g^{-1} range.[128] Ablation rates range from 0.1 to 3 mg min^{-1} depending on the element, discharge area, current, and voltage.[128] At these rates, the Grimm source is ideal for thin layer analysis or in-depth profiling where it may be necessary to profile from a few nanometers to several tens of micrometers in a relatively short time.[83] Hocquaux[83] wrote an excellent chapter on thin film analysis by GD emission spectroscopy.

The other two sources shown in Figure 9 are hollow cathode discharges. Although the hollow cathode discharge appears similar to the planar cathode physically, the shape of the cathode cavity provides some properties that make it appealing for atomic spectroscopy. This discharge derives its name from a cathode that has been drilled out to form a cylindrical cavity closed at one end.[129] The so-called hollow cathode effect can be visualized as a GD with two parallel cathode plates being brought sufficiently close to each other until the two cathode glow regions coalesce.[130] The result of this coalescence is an increase in current density that can be several orders of magnitude larger than a single planar cathode at the same cathode fall potential.[131] Coupling this increase in current density with the longer residence time that the analyte experiences in the negative glow region (owing to the cathode's shape) results in a marked increase in the intensity of radiation emitted compared to a planar cathode. In addition, background intensities are low because electron number densities are low, resulting in a very high signal-to-background ratio.[132] To perform an analysis using a hollow cathode discharge, it is necessary to machine the sample into the shape of a cylinder or to place powder or metal chips into a hollow cathode made of some inert material such as graphite. One can also analyze solutions by drying a residue on the hollow cathode surface. Operating conditions vary widely, but typically range from 200 to 500 V, 10 to 100 mA, and 0.1 to 10.0 Torr.[10] Detection limits have been reported in the picogram range,[128] but more typical results are in the nanogram range. Although hollow cathode discharges are widely used in atomic spectroscopy, the majority of these devices are light sources for AAS (see below). A typical hollow cathode lamp (HCL) is depicted at the extreme bottom right of Figure 9. Recently, Steers and coworkers compared optical emission intensities for a large number of lines over a wide spectral range in plane and hollow cathodes in a Grimm-type GD source.[133] All lines with excitation energy below 5 eV showed a higher intensity in the hollow cathode discharge, indicating that the latter could be advantageous for analytical applications. On the other hand, the asymmetric charge transfer excitation process responsible for some ion lines appeared to be suppressed in the hollow cathode discharge.

3.3 Atomic Absorption Spectroscopy

In absorption spectroscopy, spectrochemical information can be found in the magnitude of the radiant power from an external light source that is absorbed by an analyte.[122] To obtain information relevant to measuring an element's concentration, however, it is necessary for the frequency of the incident radiation to correspond to the energy difference between two electronic states of the analyte atoms being measured. Often, but not always, the atoms start in their electronic ground state and are excited to a higher lying electronic state by the incident radiation. The absorption of this radiation usually follows Equation (5):

$$A = -\log T = \frac{-\log M}{M_0} = abc \qquad (5)$$

where A is the absorbance, T the transmittance, a the absorptivity, b the path length of absorption, and c the concentration of the absorbing species. This equation is commonly referred to as *Beer's law*. To calculate the concentration, one measures the incident radiation (M_0) and the transmitted radiation (M), calculates the absorbance, and relates the absorbance to concentration using a series of standards and calibration curves, similar to emission spectroscopy.

A typical instrumental configuration for an atomic absorption spectrometer is shown in Figure 10. A hollow

Encyclopedia of Analytical Chemistry, Online © 2006–2016 John Wiley & Sons, Ltd.

This article was published in the *Encyclopedia of Analytical Chemistry* in 2016 by John Wiley & Sons, Ltd.
DOI: 10.1002/9780470027318.a5107.pub3

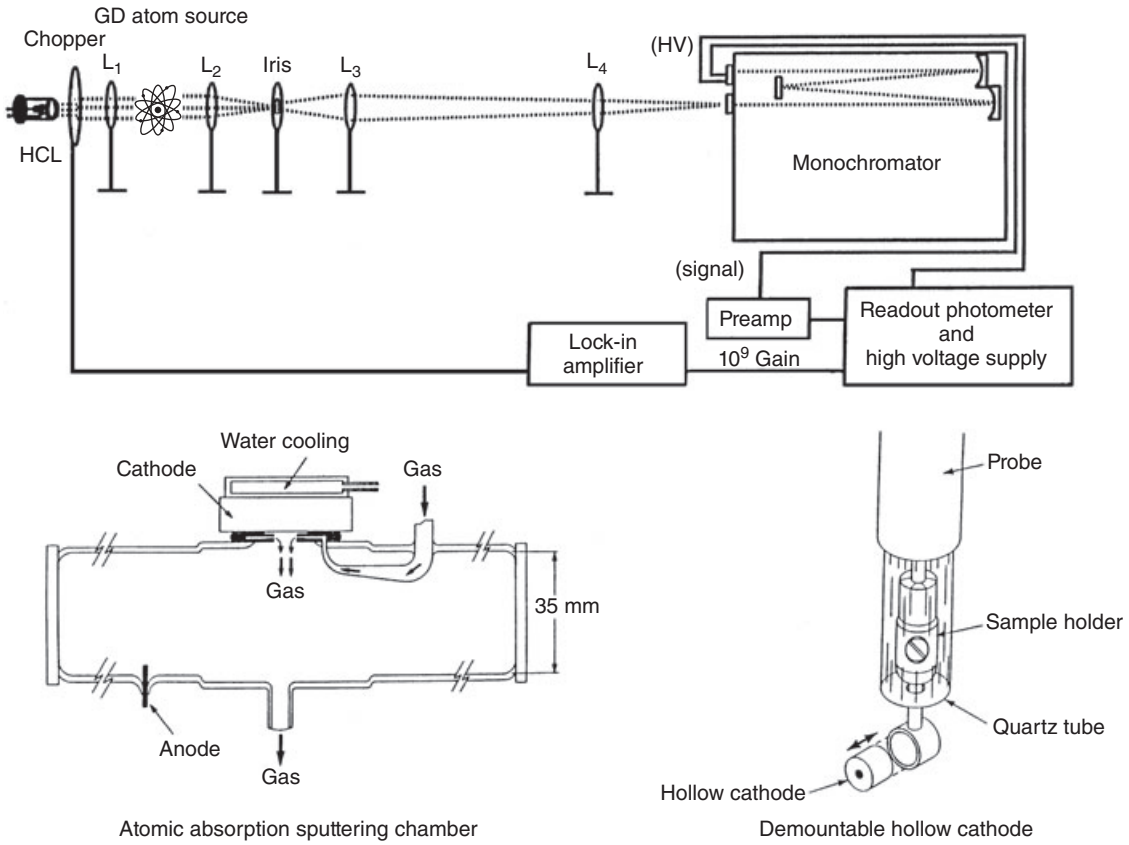

Figure 10 Schematic of an instrumental arrangement used at the Oak Ridge National Laboratory for AAS. (Reprinted with permission from D. S. Gough, Direct Analysis of Metals and Alloys by Atomic-absorption Spectrometry, *Anal. Chem.*, **48**, 1926-1931., (1976) © (1976) American Chemical Society.)

cathode, fabricated from the elements of interest, is often used as the source of incident radiation, although an electrodeless discharge lamp may be used for some elements such as As, Se, or Te, where the emission from an HCL may be low. The HCL is focused to a point inside the discharge and then refocused into the entrance aperture of the monochromator. To obtain the background signal, one can use a shutter or alternatively modulate the HCL and measure the background during the off period. In the arrangement shown in Figure 10, a mechanical chopper is used to facilitate background subtraction by providing a reference signal to a lock-in amplifier. Transmission is measured first with the discharge off and then with the discharge on, often for a range of currents and voltages. Using Beer's law, absorbance is calculated for a series of standards to produce a calibration curve; the absorbance of an unknown is then correlated with its concentration.

Two different discharge configurations are shown in Figure 10 for atomic absorption. The one on the left-hand side is an atomic absorption sputtering chamber developed by Gough.[134] A planar cathode is mounted near the top by pressing the sample against an O-ring that provides the vacuum seal. The gas flow of the cell was designed to provide transport of sputtered atoms into the observation zone, 1–2 cm from the sample. In 1987, Bernhard[135] took the idea of gas-assisted transport of atoms one step further, reporting on a design that used gas jets aimed at the sputtering surface to significantly increase the sampling rate and the absorption signal in a sputtering chamber. A commercial atomic absorption cell was designed based on this principle (Atomsource,[135] Analyte Corporation, Medford, OR), renewing the interest in AAS that began with Walsh[136] more than six decades ago. The source on the right-hand side is a much simpler atom generator. It is based on the direct insertion probe (DIP) design of King.[137] The coaxial cathode in King's original design has been replaced by a stainless steel ring that accommodates a demountable hollow cathode (4.82 mm in diameter × 2.54 mm in length with a 3.18-mm hole at the center). The DIP facilitates alignment of the HCL emission, which is focused through the orifice (i.e. the region of the highest atom density) and collected after it passes through a window in a six-way vacuum cross. Typical operating conditions for this source

Encyclopedia of Analytical Chemistry, Online © 2006–2016 John Wiley & Sons, Ltd.

This article was published in the *Encyclopedia of Analytical Chemistry* in 2016 by John Wiley & Sons, Ltd.
DOI: 10.1002/9780470027318.a5107.pub3

are 1.0–3.0 Torr, 500–2000 V, and 2–15 mA. Detection limits for GD atomic absorption are in the low-parts-per-million range. Although GD atomic absorption is not as widely used as flame or graphite furnace atomic absorption, it has found its niche in applications where analysis by other atomic absorption methods (primarily solution-based) is difficult (e.g. the analysis of materials that are difficult to dissolve).

3.4 Atomic Fluorescence Spectroscopy

Atomic fluorescence is similar to AAS in that both rely on an external light source to produce an analytical signal from an atomic vapor. In fluorescence spectroscopy, the signal is contained in the emission of photons from the atom population after absorption of the incident energy. There are five basic types of fluorescence: resonance, direct-line, step-wise, sensitized, and multiphoton fluorescence.[122] For this discussion, it is not important to define these five types, but only to say that the differences lie in the excitation and relaxation pathways that each follows to produce fluorescence. Resonance fluorescence (where the same upper and lower levels are involved in the excitation–deexcitation process so absorption and emission wavelengths are the same) finds the most widespread use in analytical spectroscopy because the transition probabilities and the source radiances are the greatest for resonance fluorescence when conventional line sources are used.

Figure 11 shows a conventional instrumental arrangement for a single-beam atomic fluorescence spectrometer. Radiation from the source is focused into the GD. Fluorescence photons are imaged onto the entrance aperture of a monochromator that isolates the analyte fluorescence from background emission and fluorescence from other species. Fluorescence is usually viewed at an angle of 90° with respect to the excitation source to minimize the collection of scattered source radiation.

One critical component of an atomic fluorescence spectrometer is the excitation source. HCLs, electrodeless discharge lamps, and metal vapor discharge lamps have all been used successfully, although today most fluorescence experiments use a laser. Lasers are superior sources for atomic fluorescence because they provide a fluence several orders of magnitude greater than other sources, are tunable over a wide wavelength range, have spectral bandwidths much narrower than absorption linewidths, and can be focused to very small spot sizes. Both continuous wave (with chopping) and pulsed lasers have been used, with dye lasers finding the most use because

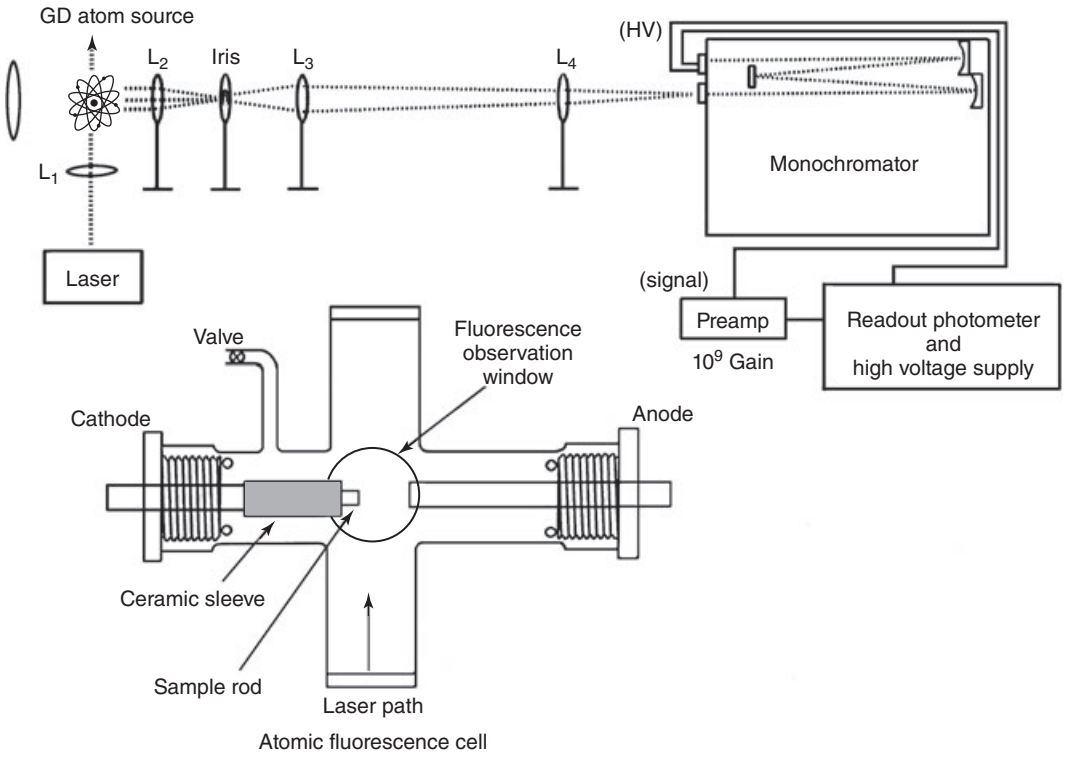

Figure 11 Schematic of a conventional instrumental arrangement for a single-beam atomic fluorescence spectrometer.

Encyclopedia of Analytical Chemistry, Online © 2006–2016 John Wiley & Sons, Ltd.

This article was published in the *Encyclopedia of Analytical Chemistry* in 2016 by John Wiley & Sons, Ltd.
DOI: 10.1002/9780470027318.a5107.pub3

they can be tuned over a large number of wavelengths. An inductively coupled plasma has also been used as an excitation source; here, the excitation wavelength is governed by the analyte that is aspirated into the torch (usually at high concentrations).

Like AES and AAS, the ideal atomizer for fluorescence would produce a stable population of atoms of sufficient number density to make quantification of small concentrations practical. A fluorescence atomizer should also produce minimum thermal excitation to limit analyte and interference emission, a potential source of background. When this stipulation is met, Rayleigh scattering from atoms or molecules determines the fundamental limitation for background noise.

Most atomic fluorescence measurements have been made with flame atomizers,[122] but recently inductively coupled plasma has been used. Plasmas generally provide better atomization efficiency and a larger population of free atoms than flames. When analyzing a solid sample, however, an atomizer, like the one shown in Figure 11, is more practical.[138] This simple design consists of a Pyrex glass housing into which a 6.35-mm diameter sample rod is inserted through a ceramic sleeve and sealed to the cell with O-rings. Quartz windows are glued into the cell to allow a laser beam to pass. A fill port and an evacuation port are also provided, and the entire cell is pumped by a single rotary vacuum pump. A DC power supply (Electronic Measurements, Eatontown, NJ) provides voltages up to 600 V and currents up to 200 mA. A typical operating voltage is 570 V at 25 mA. The cell is pressurized with argon to between 900 and 1000 Pa (7–8 Torr).

Another application of atomic fluorescence by this group[139] is based on a GD cell constructed from high vacuum components such as ConFlat® crosses and flanges with sapphire windows, but the principles of operation remain the same – fluorescence is detected 90° to the laser beam path by a photomultiplier tube. The fluorescence signal is amplified by a wideband amplifier and processed by a gated integrator and boxcar averager; the result is a fluorescence spectrum as a function of wavelength, which is indicative of those elements in a GD cathode for which a fluorescence transition is allowed.

Finally, it is worth to mention that atomic fluorescence spectrometry has also been used for diagnostic studies in a GD plasma, more specifically for measuring the 2D density profiles of sputtered Ta atoms and the corresponding ions,[140] as well as for measuring the 2D density profiles of Ar metastable atoms.[141] In both cases, a comparison was made with computer modeling results, to obtain better insights in the underlying mechanisms for production of these species in the GD, and reasonable agreement was obtained.[140,141]

3.5 Optogalvanic Spectroscopy

The final optical technique to be discussed is optogalvanic spectroscopy. The optogalvanic effect was first observed using a weak, incoherent light source in 1928[142]; light from one neon discharge affected the electrical characteristics of a nearby discharge. The process is quite simple; in a discharge there is an equilibrium established between the neutral species and the corresponding ions. If some means of energy is added to the discharge, the equilibrium position can be displaced and the fraction of ions altered; this is the case when a photon is absorbed by the gaseous atom or molecule. This permits one to measure optical absorption by an all-electronic means, that is, without the use of photodetectors. The electrical circuit employed to monitor the optogalvanic effect commonly includes a ballast resistor in series with the discharge resistance; the discharge impedance change is usually monitored as a change in the discharge voltage. The light source is modulated, and a lock-in amplifier is employed to measure the alternating current component of the discharge voltage induced by absorption of light as the source wavelength is scanned. In theory, the atomization source could be any of the discharges discussed so far; in practice, however, we have found that the demountable hollow cathode operating in the same manner as it does for atomic absorption provides the greatest flexibility for optogalvanic spectroscopy.[143]

4 MASS SPECTROMETRIC METHODS OF ANALYSIS

Much like the spectrochemical techniques described above, mass spectrometry offers the analyst a method for determining the identity and quantity of a particular species in a sample. This technique, however, provides analytical information through the separation and subsequent detection of charged species associated with the sample. Ions are generated in the source region and selected by mass-to-charge ratio (m/z) usually using electrostatic or magnetic fields.

In this section, the basic requirements necessary to obtain mass abundance information are described, along with five types of mass spectrometers: quadrupole mass filters, magnetic sector mass analyzers, QITs, FTICR devices, and TOF mass spectrometers. This article focuses only on variants that have been coupled to the GD source. Table 4 provides basic information and characteristics that are unique to each of the mass spectrometric systems.

Encyclopedia of Analytical Chemistry, Online © 2006–2016 John Wiley & Sons, Ltd.

This article was published in the *Encyclopedia of Analytical Chemistry* in 2016 by John Wiley & Sons, Ltd.
DOI: 10.1002/9780470027318.a5107.pub3

Table 4 Mass analyzers and considerations for elemental analysis

Mass analyzer type	Advantages	Disadvantages
Magnetic sector mass spectrometer	Commercially available Reasonable resolution	Scan speed Complex Cost
Quadrupole mass filter	Commercially available Robustness Scan speed Peak hopping mode	Limited resolution
QIT mass spectrometer	Cost Collision-induced dissociation (CID) to remove interferences	Complicated interface to GD source Cost
FTICR mass spectrometer	High resolution CID capability	Complex Complicated interface to GD source Space charge limited
TOF mass spectrometer	Simplicity Cost Speed Simultaneous data acquisition Good resolution when operated in reflectron mode Source space charge limited	Some ion extraction biases Poor isotope ratio measurements

4.1 Basic Requirements Necessary to Obtain Mass Abundance Information

Mass spectrometric systems in general require a number of fundamental components to create, transport, separate, and detect ions, manipulate the resulting signal to account for system inconsistencies, and provide useful information to the analyst (Figure 12). A number of these components are considered in the following section.

4.1.1 Ion Source

There are a number of GD source geometries that can be implemented for a variety of analyses (Table 1). Some types were designed, and are well suited, for optical applications as outlined in the previous section. Many of the advantages afforded by the optically applicable sources stem from an enhancement of the atom population, often a result of increased sputtering rate or a confined viewing region that facilitates optical viewing. However, mass spectrometry requires a different set of criteria. Sources designed for mass spectrometric applications must provide a reasonable population of analyte ions (not atoms). These ions must then be extracted from the source region into the mass analyzer. For these reasons, one appropriate source for mass spectrometry is the coaxial cathode. Ions generated by the coaxial cathode are extracted through an ion exit orifice in the anode. Ionization is dominated by the Penning process that leads to an ion population with a narrow KE spread relative to other GD source geometries.[144] This geometry also facilitates sample introduction via a DIP, making the appropriate adjustment of the plasma relative to the ion exit orifice trivial. On the other hand, Grimm-type sources have also been more and more combined with mass spectrometric detection in the last decades.

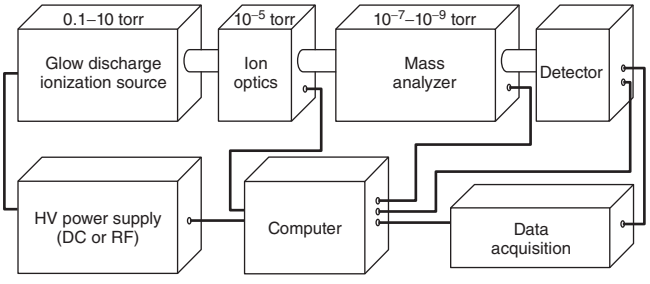

Figure 12 Block diagram of typical GD mass spectrometer system components.

4.1.2 Vacuum Systems

Mass spectrometric techniques impose stringent requirements on a vacuum system. One advantage of interfacing any of the currently available mass analyzers to the GD as compared to an atmospheric pressure source arises from the operating pressure of the ion source itself. Most mass spectrometers operate at pressures from 10^{-5} to 10^{-9} Torr. The GD source also operates at a reduced pressure (0.1–10 Torr with support gas), although not nearly as low as those required for mass analysis. The pressure differences associated with GD mass spectrometric implementation are overcome using differential

Encyclopedia of Analytical Chemistry, Online © 2006–2016 John Wiley & Sons, Ltd.

This article was published in the *Encyclopedia of Analytical Chemistry* in 2016 by John Wiley & Sons, Ltd.
DOI: 10.1002/9780470027318.a5107.pub3

pumping schemes. These types of systems employ a series of pumping regions to reduce the effect of the required pressure drop. A typical scheme would involve pumping the ion source with a rotary vane roughing pump. This would evacuate the discharge cell to a pressure of approximately 10^{-3} Torr in the absence of discharge gas. The next differentially pumped region facilitates extraction of ions from the ion source. This region is often evacuated using a turbomolecular pump or oil diffusion pump and maintains pressures of 10^{-4}–10^{-5} Torr during discharge operation. The analyzer region, which includes the mass separation components as well as the detector, is evacuated using a turbo molecular, oil diffusion, cryo, or ion pump and maintains pressures of 10^{-7}–10^{-9} Torr.

4.1.3 Ion Optics

Ions generated in the GD plasma must be transported efficiently and indiscriminately to the mass separation region to facilitate accurate and precise analytical measurements. The transfer of ions from the source to the mass analyzer is usually accomplished using an optics system. One type of system used for ion transport is the Einzel lens.[18,145,146] This type of lens is based on three conducting tubular lenses of similar dimension mounted in series. Typically, similar potentials are placed on the first and third lenses while that of the middle lens is adjustable. Many times the middle lens is held at ground potential. As an ion beam passes through this lens system, it is focused in a manner analogous to an optical beam, reaching a focal point on the opposite side. It is important to note that cylindrical lens systems such as the Einzel lenses produce a cylindrical ion beam rather than a planar one. This characteristic may limit their use for some applications such as ion guides for magnetic sector instruments that require a ribbon-shaped ion beam.

A second type of ion optic is the Bessel box.[147,148] This technology is used in conjunction with QMAs to remove photons and neutral species from the ion beam while simultaneously limiting the KE spread of ions entering the quadrupole lens region. If the energy spread is very large, quadrupole performance deteriorates, resulting in degradation of mass resolution, peak splitting, and asymmetrical peak shapes.[149,150] A Bessel box is constructed from a square entrance and exit electrode surrounded by sets of electrodes on each of the other four sides. A center plate or cone is located within the box parallel to the entrance and exit electrodes. Potentials are applied to each electrode. These potentials can be varied to permit the transmission of ions with a discrete KE. Photons and neutral species will not be affected by these potentials and will proceed into the box linearly and collide with the center stop, removing them from the beam. Ions entering the box with very little KE will be repelled toward the entrance plate. If the energy of the ion is very large, it will not be steered around the center stop and will collide with the side electrode or exit plate. Only ions with the selected KE will travel around the center stop, through the exit aperture, and into the quadrupole region. In most cases, one or two lenses are located behind the exit aperture to focus and transport the selected ions.

Quadrupole lenses can also be used as ion guides when operated in an RF-only mode.[151,152] It is shown later in this article that the application of both DC and RF potentials provides a notch filter that can be adjusted and scanned to provide mass unit resolution. When only an RF potential is applied, the quadrupole acts as an ion guide, focusing all ions through quadrupole lenses.

4.1.4 Detection Systems

Three types of detection systems are routinely used for GD mass spectrometric measurements: Faraday cups, electron multipliers, and microchannel plates (MCPs). Detector selection is often independent of the mass analyzer in use.

The detector used most often for applications with high ion abundance is the Faraday cup. Modern Faraday detectors are extremely quiet. When operated using high-grade resistors and amplification components, these detection systems offer state-of-the-art measurements with respect to signal-to-noise ratio. Although not currently available on commercial GD mass spectrometric systems, recent developments in multi-Faraday array detection systems offer increasingly precise measurements for scanning instruments by negating the effects of source fluctuations on measurements. Each Faraday cup in the array is dedicated and positioned to measure a single isotope at a given dispersion setting. This allows simultaneous collection of the selected ions during the acquisition sequence without scanning the mass dispersion device, virtually removing any dependence on fluctuations in ion beam intensity arising in the source. Minimization of source fluctuation effects afforded by multicollector arrays is most important for applications involving the measurement of isotope ratios.

For applications requiring optimum sensitivity, discrete dynode electron multipliers operated in a pulse-counting mode are required. Operation in this mode registers a signal pulse for every ion impinging on the first dynode. Each impinging ion generates a number of secondary electrons that are successively amplified by each dynode. Overall gains of 10^6–10^8 are common when using multipliers with 14–20 dynodes. After the pulse of electrons leaves the multiplier, it is amplified and proceeds to a discriminator that is set to remove pulses arising from dark noise. The signal is then sent to a universal counter

Encyclopedia of Analytical Chemistry, Online © 2006–2016 John Wiley & Sons, Ltd.

This article was published in the *Encyclopedia of Analytical Chemistry* in 2016 by John Wiley & Sons, Ltd.
DOI: 10.1002/9780470027318.a5107.pub3

that records each pulse, stores it for a given time, and passes it to a computer-based data acquisition system that presents the data in a usable form. It is important to keep the count rate low enough ($<10^6$ counts s^{-1}) to maintain the integrity of the pulse-counting system and to ensure that any pulse, not measured because of time lag in the electronics, will be statistically insignificant.

Daly detection systems behave in a manner similar to electron multipliers.[153] In the Daly system, the ion beam is accelerated to 10–20 kV and directed onto a highly polished aluminized steel electrode positioned directly behind the collector slit. Approximately eight electrons are liberated from the aluminized surface for every impinging ion. These electrons are repelled by the high negative potential applied to the electrode and directed onto a scintillator that produces a photon for each electron. These photons are counted by a photomultiplier located outside of the vacuum system. The resulting pulses are treated in a manner analogous to that of the electron multiplier. Both Daly and electron multiplier-based detection systems can be operated in a mode that integrates the current of the impinging ion beam. This mode of operation is used for applications that do not impose such stringent sensitivity requirements.

A third detection system is most often used with TOF instruments and is built around an MCP detector. The MCP is characterized by a large, flat active area, high gain, and excellent time response. These operating parameters make it an ideal detector for TOF mass spectrometry. These detectors are fabricated from very thin glass wafers or plates perforated with microscopic channels oriented parallel to the impinging ion beam. The nature of the detector material is such that, in the presence of a potential bias (up to 1200 V), an ion impinging on the entrance to one of the channels will liberate one or more electrons, which will, in turn, cascade through the channel, liberating further electrons with each wall collision. Amplification of the order of 10^4 is routinely realized for a single MCP. After they emerge from the MCP, these electrons are collected by a positively charged electrode positioned parallel to the MCP. The resulting signal is further amplified and manipulated using a fast digitizing oscilloscope or any number of computer-based flash analog-to-digital converter (ADC) computer boards. Two or more MCPs can be arranged in a stack orientation to further amplify the signal, thus increasing the system's performance.

4.2 Magnetic Sector Mass Analyzers

Initially used by Aston[154] for his studies of gaseous discharges, the magnetic sector mass analyzer, or mass spectrograph as Aston called it, is based on the spatial dispersion of ions with different m/z that is effected when

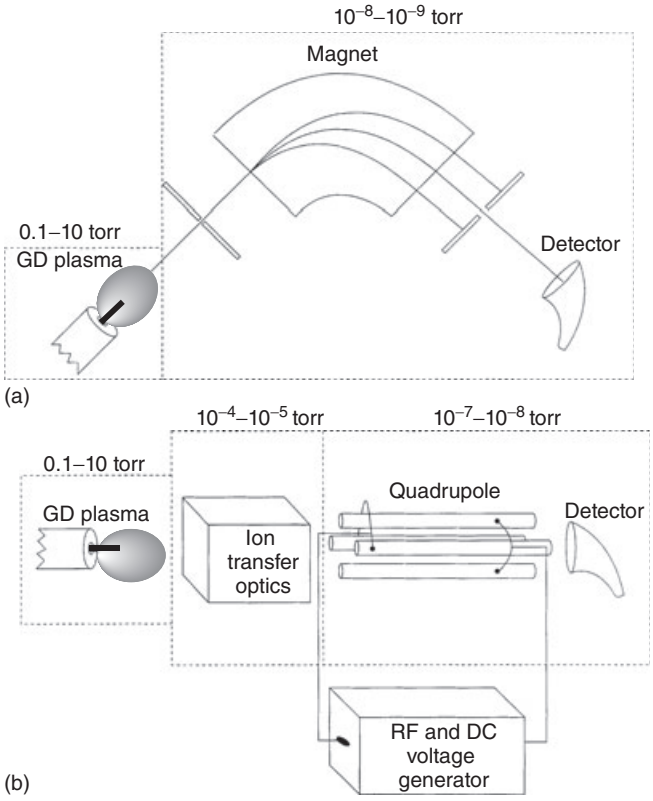

Figure 13 Schematic of (a) a magnetic sector mass spectrometer and (b) a QMA.

they traverse an electromagnetic field. The magnetic field acts as a prism dispersing monoenergetic ions of differing m/z values across a focal plane; see Figure 13(a).[155] The radius of the curved flight path of an ion through a magnetic field is given by Equation (6):

$$r_m = \left(\frac{144}{B}\right)\left(\frac{mV}{z}\right)^{1/2} \tag{6}$$

where B is the magnetic field strength in gauss, m the atomic mass of the ions (in atomic mass unit), V the acceleration voltage of the ion before it enters into the magnetic field (in volts), z the charge of the ion, and 144 a constant prescribed by the units.[155] Because a sector instrument can be made to focus ions onto a plane, it can be designed as either a single or multicollector instrument. A single electronic detector is used when operating in the sequential acquisition mode. Different m/z ions are brought into focus on the detector by varying either B or V. Simultaneous acquisition instruments utilize either a photographic plate or a detector array oriented in the focal plane. These systems allow the detection of a suite of different m/z ions at a given B and V setting. Although more expensive, the array-based

Encyclopedia of Analytical Chemistry, Online © 2006–2016 John Wiley & Sons, Ltd.

This article was published in the *Encyclopedia of Analytical Chemistry* in 2016 by John Wiley & Sons, Ltd.
DOI: 10.1002/9780470027318.a5107.pub3

systems offer shorter analysis times and the potential for more precise measurements because source fluctuation effects are minimized.

Mass resolution is another parameter that influences the ability of a system to solve an analytical problem. Mass resolution is a measure of the instrument's ability to separate ions having small mass differences. Mass resolution in magnetic sector instruments is defined by ion beam focusing at the focal plane. Single-focusing instruments rely on direction focusing to increase resolution. This is accomplished by narrowing the entrance and exit slit widths, thus reducing the width of the ion beam.[155] Mass resolution becomes more important when ions of the same nominal mass must be separated.

Multisector instruments are quite complex and expensive to build and maintain. They provide adequate-to-excellent resolving power, especially when an electrostatic sector is coupled to a magnetic sector to provide double (momentum and energy) focusing. When operated in the sequential detection mode, sector instruments are hindered by relatively slow scanning speeds that adversely affect analysis time and sample throughput. In the past, a number of commercial instruments were available from a variety of vendors based on the sector design. Currently, however, their availability has become slightly limited. Nevertheless, in 2010, Hieftje and coworkers coupled a DC GD source with a Mattauch–Herzog mass spectrometer and a third-generation Faraday strip array detector and showed that this combination provides superior resolving power and therefore improved detection limits.[156]

4.3 Quadrupole Mass Filters

Since its development in the 1950s and early 1960s, the quadrupole mass spectrometer has become a powerful tool for the analysis of a variety of materials. Much of its popularity stems from the time of its development when it was viewed as a more rugged, more compact, and more cost-effective alternative to magnetic sector mass spectrometry systems, albeit with compromised performance. The quadrupole mass filter is a variable bandpass filtering ion optic, analogous to an optical bandpass filter. The quadrupole system is capable of transmission of all ions when operated in the RF-only mode (as described earlier) or of measuring only one m/z at a time as a sequential mass analyzer. The quadrupole offers the ability to scan the entire mass range very rapidly or to 'peak-hop' among a series of selected isotopes.[157] A quadrupole mass filter consists of four high-precision, cylindrical, conducting rods or poles arranged in a square configuration, as shown in Figure 13(b). Mass filtering is accomplished by applying steady-state DC and pulsed RF potentials to these poles. The application of these voltages results in the formation of hyperbolic electric fields, with the ideal quadrupole defined by Equation (7):

$$\frac{r}{r_0} = 1.148 \tag{7}$$

where r is the radius of each rod and r_0 the radius enclosed by the electrodes.[158] The effects that the applied potentials and resulting electric fields have on a charged particle are best described by the ion trajectory in the $x–z$ and $y–z$ planes. The set of poles in the $x–z$ plane have a positive, time-independent DC voltage and a time-dependent RF voltage applied to them. The poles in the $y–z$ plane have a negative, time-independent DC voltage and a time-dependent RF voltage applied to them. The RF potential applied in the $y–z$ plane is 180° out of phase with the RF voltage in the $x–z$ plane. Ions enter and travel between the poles along the z-axis.

In the $x–z$ plane, larger mass ions are focused along the z-axis by the positively biased DC field, while the smaller mass ions are destabilized by the RF field. In the $y–z$ plane, larger mass ions are deflected away from the z-axis by the negatively biased potential while ions of smaller masses are stabilized by the RF field. The net result is a high-pass filter in the $x–z$ plane and a low-pass filter in the $y–z$ plane, allowing the stabilization and transmission of ions above a selected m/z, and the stabilization and transmission of ions below a selected m/z, respectively. When these two types of filters coexist, a narrow bandpass mass filter results. The magnitude of the DC potential and the frequency of the RF potential can be varied to allow transmission of different m/z ions through the quadrupole lenses, thus providing a means of m/z selection.

Quadrupole-based GD systems have been used extensively.[42,43] The relatively low cost and robustness of these instruments have made them an excellent choice for both the researcher and routine sample analyst. A major limitation of the quadrupole system is its relatively low resolving power, significantly increasing the deleterious effects of overlapping polyatomic interferences. Appropriate selection of operating conditions and discharge gas can minimize some of these concerns, but the performance of quadrupoles does not match that of sector-based instruments.

4.4 Ion Trap and Fourier Transform Ion Cyclotron Resonance Devices

While sector and QMAs were being developed for elemental and isotopic applications, the QIT technology was being driven by needs in the organic community. FTICR mass spectrometry, another form of ion trapping technology, has filled a niche in the biological mass

Encyclopedia of Analytical Chemistry, Online © 2006–2016 John Wiley & Sons, Ltd.

This article was published in the *Encyclopedia of Analytical Chemistry* in 2016 by John Wiley & Sons, Ltd.
DOI: 10.1002/9780470027318.a5107.pub3

spectrometry community because of its unrivaled mass resolution.[159] Recently, these devices have been characterized and used by the inorganic mass spectrometric community. A number of external ionization sources have been implemented, including the GD.[159,160] This section describes the operating principles of both the QIT and FTICR systems and covers some of their unique properties.

The operation of the QIT is very similar to that of the quadrupole mass filter. Two of the opposing rods in the quadrupole mass filter are connected to form a ring, and each of the remaining pair of rods is replaced by a hyperbolic end-cap, as shown in Figure 14(a). The result is a three-dimensional quadrupole field that is symmetric with respect to rotation about the center. The end-caps are oriented along the former z-axis, and the x- and y-axes become a plane, r, symmetric about z. In the most common inorganic applications, externally generated ions are collected and stored within the trap. Typically the internal pressure of the QIT is 10^{-3}–10^{-4} Torr He. Helium is introduced to cool collisionally the precessing ions, thus allowing them to relax toward the center of the trap and increase trapping efficiency.

Stored ions precess with a frequency that is m/z dependent. Ions that are stored in the trapping fields have a fundamental secular frequency along the axial or z-axis. When a supplemental AC signal is applied to the end-cap electrodes, ions whose secular frequencies are in resonance with the applied frequency are excited to higher translational energies. The magnitude of this resonance excitation is directly proportional to the amplitude of the applied signal. At appropriately high amplitudes, the ions can either be lost in collisions with an electrode or be ejected through apertures in the exit end-cap electrode. Mass analysis can thus be performed by scanning the frequency of the AC excitation signal. During a scan, ions become destabilized through the excitation process and are selectively ejected through the exit end-cap electrode and are then detected using an electron multiplier.

The relatively high operating pressure of the QIT makes it well suited for coupling to ion sources that operate at higher pressures, such as the GD. Ions from the GD can be directly introduced into the QIT without the need for an elaborate differential pumping scheme. The high pressure and trapping nature of the QIT also facilitate the use of ion–molecule interactions to provide a number of advantageous results, most notably the suppression of unwanted contributions from isobaric interferences.

The FTICR mass spectrometer was initially considered by the elemental mass spectrometry community for its high resolving power. This characteristic allows the physical separation of the analyte signal from interferences without actually removing the interfering

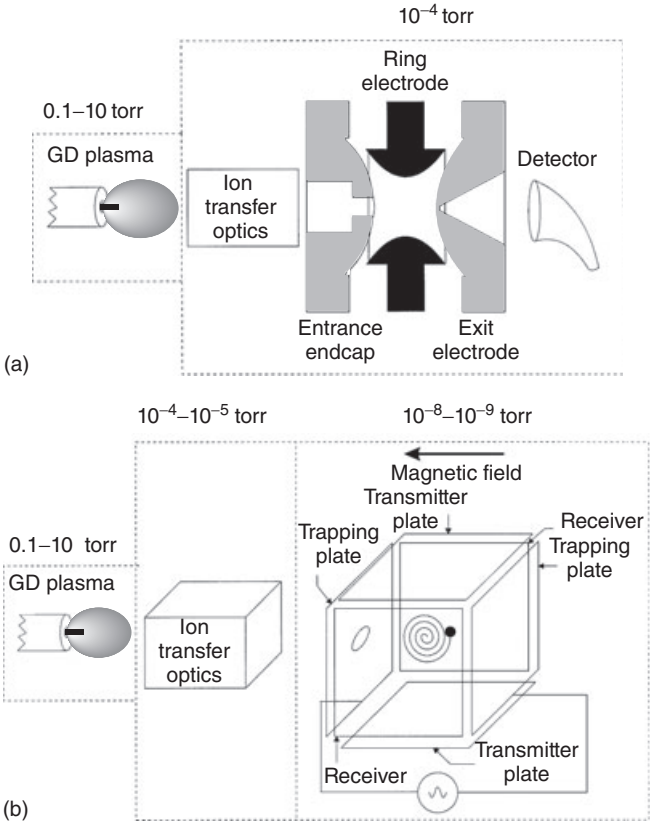

Figure 14 Schematic of (a) a QIT mass spectrometer and (b) an FTICR mass spectrometer.

species from the cell. However, high resolution does not come without a cost: FTICR systems are one of the most expensive types of mass spectrometers available. The basic operation of the FTICR system is similar to that of the QIT. Precessing ions are constrained spatially within a cubic cell using both electric and magnetic fields. A homogeneous magnetic field confines ions radially, while electrostatic potentials are applied to the end-caps of the cell to trap the ions axially; see Figure 14(b). Ions trapped by these fields are characterized by three motions: one that confines the ions between the two end-cap electrodes, magnetron motion, and cyclotron motion.[161] The ions orbit perpendicular to the applied magnetic field at the ion characteristic cyclotron frequencies, T_c, that are inversely proportional to their m/z values and proportional to the magnetic field strength, B,[162] as shown in Equation (8):

$$w_e = \frac{zB}{m} \tag{8}$$

Ions are excited to larger cyclotron orbits by the application of a resonant RF potential to transmitter

Encyclopedia of Analytical Chemistry, Online © 2006–2016 John Wiley & Sons, Ltd.

This article was published in the *Encyclopedia of Analytical Chemistry* in 2016 by John Wiley & Sons, Ltd.
DOI: 10.1002/9780470027318.a5107.pub3

plates. An image current is generated as the coherent ion packets of a given m/z come into close proximity to the receiver electrodes. This current is converted to a voltage, amplified, digitized, and stored as a transient signal. The Fourier transform converts these transient signals into their frequency components, T_c, which are, in turn, related to the m/z as shown in Equation (8). Extremely high mass resolution can be achieved because the basis for mass measurement lies in measuring frequency, which can be done with great precision.[163] It should also be noted that mass resolving power is inversely proportional to the ion m/z,[164] a fortunate circumstance for elemental analysis because all masses of interest are below 250 Da.

4.5 Time-of-Flight Mass Spectrometers

Perhaps the simplest type of mass spectrometer, the TOF mass spectrometer, is depicted in Figure 15. Its operation is based on the KE equation, where KE is a function of mass, m, and velocity, v; alternatively, it can be expressed in terms of charge, z, and accelerating potential, V, as shown in Equation (9):

$$\mathrm{KE} = \frac{1}{2}mv^2 = zV \tag{9}$$

From this equation, one can deduce that ions of different m/z accelerated to a common KE will have different velocities. The TOF instrument operates on the principle that if all ions leave the extraction grid at the same point in space and time with equal KEs, they will travel with different velocities, v_y, that are inversely proportional to their respective masses, m_y, as shown in Equation (10):

$$v_y = \left(\frac{2\mathrm{KE}}{m_y}\right)^{1/2} \tag{10}$$

The time needed to traverse the flight path distance D and to arrive at the detector is related to the m_y/z ion by Equation (11):

$$t_y = D\left(\frac{m_y}{2zV}\right)^{1/2} \tag{11}$$

Monitoring the current at the detector (often an MCP) yields a time-dependent signal that can be correlated to the m/z using Equation (11). Mass resolution is directly determined from the temporal resolution At/t, which is determined by the initial KE spread of the ions and the speed of the detection electronics.

The effects of this spread in initial energy can be minimized using a reflectron TOF mass spectrometric instrument. This instrument geometry has a series of electrostatic lenses located at the end of the flight tube.

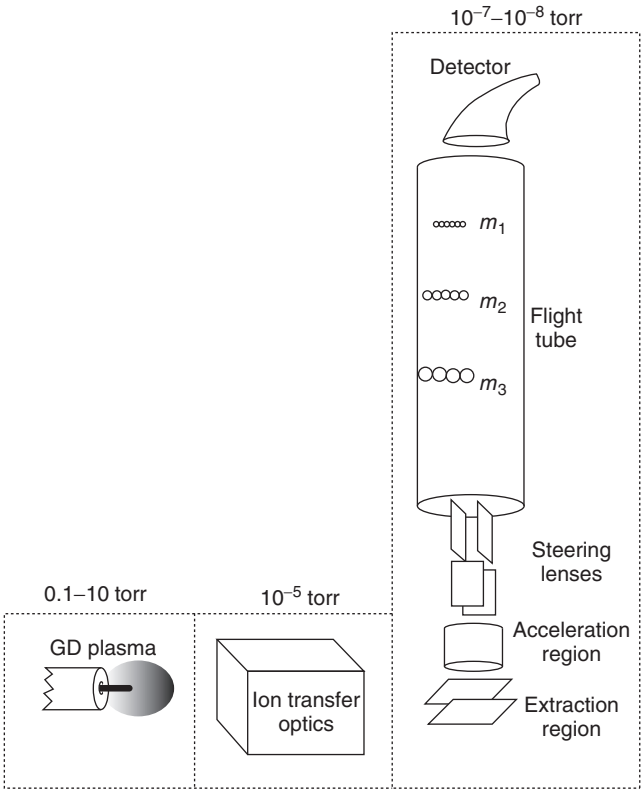

Figure 15 Schematic of a TOF mass spectrometer.

Positive potentials applied to these lenses increase toward the detection end of the flight tube. Ions traveling down the flight tube enter this potential gradient and penetrate, slowing until they reach a point in the gradient equal to their initial KE. They are then accelerated in the opposite direction, traversing the flight tube for the second time. They are then detected by an MCP located at the base of the flight tube. Ions of higher KE penetrate further into the reflectron field, increasing their flight distance (time) and effectively minimizing the impact on mass resolution.

TOF instruments are ideally suited for pulsed ion sources such as lasers or pulsed ion beam sputtering. SIMS using TOF technology has gained wide acceptance as a technique for the characterization of a wide variety of materials. TOF mass spectrometry is also well suited for use with the pulsed GD source.[61] The TOF mass spectrometer provides simultaneous detection of all ions with each injection pulse. This quality affords an excellent diagnostic tool for plasmas and is essential for the temporal characterization of millisecond and microsecond GD pulses.[61,165] Furthermore, by means of the detection of negative ions from a pulsed RF-GD, elemental and molecular analysis of halogen-containing samples by GD-TOF-MS was possible.[69]

Encyclopedia of Analytical Chemistry, Online © 2006–2016 John Wiley & Sons, Ltd.

This article was published in the *Encyclopedia of Analytical Chemistry* in 2016 by John Wiley & Sons, Ltd.
DOI: 10.1002/9780470027318.a5107.pub3

In recent years, many papers have been published on the use of (RF/pulsed) GD-TOF-MS for various applications (Section 2.4). Pereiro et al. presented a nice review paper on GD-TOF-MS, focusing on instrument developments and recent applications, both for the elemental and molecular direct solid analyses of materials and for analytes in gaseous phase (including as detector for gas chromatography). The authors also evaluated pulsed versus continuous GD-TOF-MS for elemental analysis. Applications for elemental analysis of thin films and for molecular analysis (including polymers and solid-state metal speciation) were illustrated. Quantification by GD-TOF-MS was discussed, as well as alternatives to conventional GD-TOF-MS, including magnetically boosted GD sources, alternative discharge gases, and combined laser ablation (LA) GD-TOF-MS.[166] Finally, TOF-MS was also used to study the effects of oxygen addition on the ion signals in GDMS, providing information on the fundamental processes in the GD and flowing afterglow.[167]

5 CONCLUSIONS

Optical and mass spectrometric techniques using GD ion sources are established as routine methods for the direct analysis of solid samples of widely different origin and composition, and they are also gaining increasing interest for gas and liquids analysis. This article has focused on the fundamental operation of the GD source in a number of operating modes as well as the optical and mass spectrometric instrumentation used for elemental determination. These source–instrument combinations will undoubtedly continue to offer advantages essential for specific applications in the future.

DISCLAIMER

Los Alamos National Laboratory, an affirmative action/equal opportunity employer, is operated by the University of California for the US Department of Energy under contract W-7405-ENG-36. By acceptance of this article, the publisher recognizes that the US Government retains a nonexclusive, royalty-free license to publish or reproduce the published form of this contribution, or to allow others to do so, for US Government purposes. Los Alamos National Laboratory requests that the publisher identify this article as work performed under the auspices of the US Department of Energy. Los Alamos National Laboratory strongly supports academic freedom and a researcher's right to publish; as an institution, however, the Laboratory does not endorse the viewpoint of a publication or guarantee its technical correctness.

ABBREVIATIONS AND ACRONYMS

AAS	Atomic Absorption Spectroscopy
ADC	Analog-to-Digital Converter
AES	Atomic Emission Spectroscopy
AFS	Atomic Fluorescence Spectroscopy
CID	Collision-induced Dissociation
DIP	Direct Insertion Probe
FTICR	Fourier Transform Ion Cyclotron Resonance
GD	Glow Discharge
HCL	Hollow Cathode Lamp
ICPMS	Inductively Coupled Plasma Mass Spectrometry
IR	Infrared
KE	Kinetic Energy
MCP	Microchannel Plate
QIT	Quadrupole Ion Trap
QMA	Quadrupole Mass Analyzer
RF	Radiofrequency
SIMS	Secondary Ion Mass Spectrometry
TOF	Time-of-Flight
UV	Ultraviolet

RELATED ARTICLES

Coatings
Atomic Spectroscopy in Coatings Analysis

Environment: Trace Gas Monitoring
Laser Mass Spectrometry in Trace Analysis

Environment: Water and Waste
Atomic Fluorescence in Environmental Analysis • Inductively Coupled Plasma Mass Spectrometry in Environmental Analysis • Laser Ablation Inductively Coupled Plasma Spectrometry in Environmental Analysis • Luminescence in Environmental Analysis • Optical Emission Inductively Coupled Plasma in Environmental Analysis

Forensic Science
Atomic Spectroscopy for Forensic Applications • Mass Spectrometry for Forensic Applications

Encyclopedia of Analytical Chemistry, Online © 2006–2016 John Wiley & Sons, Ltd.

This article was published in the *Encyclopedia of Analytical Chemistry* in 2016 by John Wiley & Sons, Ltd.
DOI: 10.1002/9780470027318.a5107.pub3

Atomic Spectroscopy
Inductively Coupled Plasma-Optical Emission Spectrometry • Laser Ablation in Atomic Spectroscopy

Mass Spectrometry
Mass Spectrometry: Overview and History • High-resolution Mass Spectrometry and its Applications • Inorganic Substances, Mass Spectrometric in the Analysis of • Isotope Ratio Mass Spectrometry • Literature of Mass Spectrometry • Quadrupole Ion Trap Mass Spectrometer • Tandem Mass Spectrometry: Fundamentals and Instrumentation • Time-of-flight Mass Spectrometry

REFERENCES

1. F. Paschen, 'Bohrs Heliumlinien', *Ann. Phys.*, **50**, 901–940 (1916).
2. H. Schuler, 'Uber die Anregung von Spektren zur Untersuchung von Hyperfeinstrukturen', *Z. Phys.*, **59**, 149–153 (1929).
3. H. Schuler, J.E. Keystone, 'Hyperfeinstrukturen und Kernmomente des Quecksilbers', *Z. Phys.*, **72**, 423–441 (1931).
4. A. Bogaerts, E. Neyts, R. Gijbels, J. van der Mullen, 'Gas Discharge Plasmas and their Applications', *Spectrochim. Acta Part B*, **57**, 609–658 (2002).
5. B. Chapman, *Glow Discharge Processes, Sputtering and Plasma Etching*, John Wiley & Sons, Inc, New York, 1980.
6. A.M. Howaston, *An Introduction to Gas Discharges*, 2nd edition, Pergamon Press, New York, 1976.
7. F.L. King, J. Teng, R.E. Steiner, 'Glow Discharge Mass Spectrometry: Trace Elemental Determinations in Solid Samples', *J. Mass Spectrom.*, **30**, 1061–1075 (1995).
8. W. Grimm, 'Eine neue Glimmentladungslampe fur die Optische Emissionsspektralanalyse', *Spectrochim. Acta Part B*, **23**, 443–454 (1968).
9. R.K. Marcus (ed), *Glow Discharge Spectroscopies*, Plenum Press, New York, 1993.
10. W.W. Harrison, C.M. Barshick, J.A. Klingler, P.H. Ratliff, Y. Mei, 'Glow Discharge Techniques in Analytical Chemistry', *Anal. Chem.*, **62**, 943A–949A (1990).
11. R.K. Marcus, T.R. Harville, Y. Mei, C.R. Shick, 'RF-powered Glow-discharges: Elemental Analysis Across the Solids Spectrum', *Anal. Chem.*, **66**, 902A–911A (1994).
12. A. Bogaerts, R. Gijbels, 'Modeling of Glow Discharges: What can we Learn from it?', *Anal. Chem.*, **69**, A719–A727 (1997).
13. P.W.J.M. Boumans, 'Studies of Sputtering in a Glow Discharge for Spectrochemical Analysis', *Anal. Chem.*, **44**, 1219–1228 (1972).
14. N. Matsunami, Y. Yamamura, Y. Itikawa, N. Itoh, Y. Kazumata, S. Miyagawa, K. Morita, R. Shimizu, H. Tawara, 'Energy Dependence of the Ion-induced Sputtering Yields of Monoatomic Solids', *At. Data Nucl. Data Tables*, **31**, 1–80 (1984).
15. A. Bogaerts, R. Gijbels, 'Modeling of Metastable Argon Atoms in a Direct Current Glow Discharge', *Phys. Rev. A*, **52**, 3743–3751 (1995).
16. A. Bogaerts, R. Gijbels, 'Two-dimensional Model of a Direct Current Glow Discharge: Description of the Argon Metastable Atoms, Sputtered Atoms and Ions', *Anal. Chem.*, **68**, 2676–2685 (1996).
17. T.D. Mark, G.H. Nunn, *Electron Impact Ionization*, Springer-Verlag, New York, 1985.
18. L. Valyi, *Atom and Ion Sources*, John Wiley & Son, Inc, New York, 1977.
19. F.H. Field, J.L. Franklin, *Electron Impact Phenomena*, Academic Press, New York, 1970.
20. J. Delcroix, C. Ferreira, A. Richard, 'Metastable Atoms and Molecules in Ionized Gases', in *Principles of Laser Plasmas*, ed. G. Bekefi, John Wiley & Sons, Inc, New York, 159–233, 1976.
21. V.S. Bordin, Y.M. Kagan, 'Excitation of Helium in a Hollow-cathode Discharge', *Opt. Spectrosc.*, **23**, 108–110 (1967).
22. F.M. Penning, 'Uber die Erhehung der Zundspan-nung von Neon-Argon Gemischen durch Bestrahlung', *Z. Phys.*, **57**, 723–738 (1929).
23. F.M. Penning, 'Uber den Einfluss Sehr Gerginger Beimis-chungen auf die Zundspannung der Edelgase', *Z. Phys.*, **46**, 335–348 (1925).
24. D.H. Stedman, D.W. Stetser, 'Chemical Applications of Metastable Rare Gas Atoms', *Prog. React. Kinet.*, **6**, 193–238 (1971).
25. R.L. Smith, D. Serxner, K.R. Hess, 'Assessment of the Relative Role of Penning Ionization in Low-pressure Glow Discharges', *Anal. Chem.*, **61**, 1103–1108 (1989).
26. M. Saito, 'Relative Sensitivity Factors in Direct Current Glow Discharge Mass Spectrometry Using Kr and Xe Gas – Estimation of the Role of Penning Ionization', *Fresenius J. Anal. Chem.*, **351**, 148–153 (1995).
27. A. Bogaerts, R. Gijbels, 'Role of Sputtered Cu Atoms and Ions in a Direct Current Glow Discharge: Combined Fluid and Monte Carlo Model', *J. Appl. Phys.*, **79**, 1279–1286 (1996).
28. A. Bogaerts, R. Gijbels, 'Relative Sensitivity Factors in Glow Discharge Mass Spectrometry: The Role of Charge Transfer Ionization', *J. Anal. At. Spectrom.*, **11**, 841–847 (1996).
29. A. Bogaerts, K.A. Temelkov, N.K. Vuchkov, R. Gijbels, 'Calculation of Rate Constants for Asymmetric Charge Transfer, and their Effect on Relative Sensitivity Factors

Encyclopedia of Analytical Chemistry, Online © 2006–2016 John Wiley & Sons, Ltd.

This article was published in the *Encyclopedia of Analytical Chemistry* in 2016 by John Wiley & Sons, Ltd.
DOI: 10.1002/9780470027318.a5107.pub3

in Glow Discharge Mass Spectrometry', *Spectrochim. Acta Part B*, **62**, 325–336 (2007).

30. I. Korolov, G. Bano, Z. Donko, A. Derzsi, P. Hartmann, 'Experimental Study of the Asymmetric Charge Transfer Reaction between Ar^+ Ions and Fe Atoms', *J. Chem. Phys.*, **134**, 064308 (2011).
31. I. Korolov, G. Bano, Z. Donko, 'Experimental Investigation of the Asymmetric Charge Exchange Reaction in the Ar^+-Ni System in the Afterglow of a Pulsed Glow Discharge', *Spectrochim. Acta Part B*, **66**, 706–711 (2011).
32. A. Bogaerts, R. Gijbels, 'The Role of Fast Argon Ions and Atoms in the Ionization of Argon in a Direct Current Glow Discharge: A Mathematical Simulation', *J. Appl. Phys.*, **78**, 6427–6431 (1995).
33. S. De Gendt, W.W. Harrison, 'Parameter Evaluation for the Analysis of Oxide-based Samples with Radio-frequency Glow Discharge Mass Spectrometry', *Anal. Chem.*, **67**, 1026–1033 (1995).
34. C. Lazik, R.K. Marcus, 'Effect of Excitation-frequency on Source Characteristics in Radio-frequency Glow-discharge Atomic-emission Spectrometry, 1.2–30 MHz', *Spectrochim. Acta Part B*, **49**, 649–663 (1994).
35. D.C. Duckworth, D.L. Donohue, D.H. Smith, T.A. Lewis, R.K. Marcus, 'Design and Characterization for a Radio-frequency-powered Glow-discharge Source for Double-focusing Mass Spectrometers', *Anal. Chem.*, **65**, 2478–2484 (1993).
36. J. Teng, C.M. Barshick, D.C. Duckworth, S.J. Norton, D.H. Smith, F.L. King, 'Factors Influencing the Quantitative Determination of Trace Elements in Soils by Glow-discharge Mass Spectrometry', *Appl. Spectrosc.*, **49**, 1361–1366 (1995).
37. D.C. Duckworth, C.M. Barshick, D.A. Bostick, D.H. Smith, 'Direct Measurement of Uranium Isotopic-ratios in Soils by Glow-discharge Mass Spectrometry', *Appl. Spectrosc.*, **47**, 243–245 (1993).
38. D.C. Duckworth, C.M. Barshick, D.H. Smith, 'Analysis of Soils by Glow-discharge Mass Spectrometry', *J. Anal. At. Spectrom.*, **8**, 875–879 (1993).
39. A. Bogaerts, R. Gijbels, W. Goedheer, 'Improved Hybrid Monte Carlo–fluid Model for the Electrical Characteristics in an Analytical Radio-frequency Glow Discharge in Argon', *J. Anal. At. Spectrom.*, **16**, 750–755 (2001).
40. A. Bogaerts, L. Wilken, V. Hoffmann, R. Gijbels, K. Wetzig, 'Comparison of Modeling Calculations with Experimental Results for rf Glow Discharge Optical Emission Spectrometry', *Spectrochim. Acta Part B*, **57**, 109–119 (2002).
41. D.C. Duckworth, R.K. Marcus, 'Radio-frequency Powered Glow Discharge Atomization Ionization Source for Solids Mass Spectrometry', *Anal. Chem.*, **61**, 1879–1886 (1989).
42. F.L. King, C. Pan, 'Time-resolved Studies of Ionized Sputtered Atoms in Pulsed Radio-frequency Powered Glow-discharge Mass Spectrometry', *Anal. Chem.*, **65**, 3187–3193 (1993).
43. J.A. Klingler, P.J. Savickas, W.W. Harrison, 'The Pulsed Glow-discharge as an Elemental Ion-source', *J. Am. Soc. Mass Spectrom.*, **1**, 138–143 (1990).
44. J.A. Klingler, C.M. Barshick, W.W. Harrison, 'Factors Influencing Ion Signal Profiles in Pulsed Glow-discharge Mass-spectrometry', *Anal. Chem.*, **63**, 2571–2576 (1991).
45. M.R. Winchester, R.K. Marcus, 'Emission Characteristics of a Pulsed, Radio-frequency Glow Discharge Atomic Emission Device', *Anal. Chem.*, **64**, 2067–2074 (1992).
46. M. Glick, B.W. Smith, J.D. Winefordner, 'Laser-excited Atomic Fluorescence in a Pulsed Hollow-cathode Glow Discharge', *Anal. Chem.*, **62**, 157–161 (1990).
47. W.W. Harrison, W. Hang, X. Yan, K. Ingeneri, C. Schilling, 'Temporal Considerations with a Microsecond Pulsed Glow Discharge', *J. Anal. At. Spectrom.*, **12**, 891–896 (1997).
48. W.W. Harrison, 'Pulsed Glow Discharge as a Solids Analysis Source', *J. Anal. At. Spectrom.*, **13**, 1051–1056 (1998).
49. W.W. Harrison, C. Yang, E. Oxley, 'Pulsed Glow Discharge: Temporal Resolution in Analytical Spectroscopy', *Anal. Chem.*, **73**, 480A–487A (2001).
50. C. Pan, F.L. King, 'Ion Formation Processes in the Afterpeak Time Regime of Pulsed Glow Discharge Plasmas', *J. Am. Soc. Mass Spectrom.*, **4**, 727–732 (1993).
51. C. Yang, W.W. Harrison, 'Investigation of a Novel Hollow Cathode Configuration for Grimm-type Glow Discharge Emission', *Spectrochim. Acta Part B*, **56**, 1195–1208 (2001).
52. W.W. Harrison, K.R. Hess, R.K. Marcus, F.L. King, 'Glow-discharge Mass-spectrometry', *Anal. Chem.*, **58**, 341A–356A (1986).
53. M.A. Biondi, 'Studies of the Mechanism of Electron-ion Recombination', *Phys. Rev.*, **129**, 1181–1188 (1963).
54. M.A. Biondi, 'Diffusion, De-excitation and Ionization Cross-sections for Metastable Atoms', *Phys. Rev.*, **88**, 660–665 (1952).
55. G. Lotito, T. Nelis, P. Guillot, D. Günther, 'Characterization of Argon Metastable Species as a Function of Time, Space and Current of a Pulsed Direct Current Glow Discharge', *Spectrochim. Acta Part B*, **66**, 619–626 (2011).
56. G.P. Jackson, C.L. Lewis, S.K. Doorn, V. Majidi, F.L. King, 'Spectral, Spatial and Temporal Characterization of a Millisecond Pulsed Glow Discharge: Metastable Argon Atom Production', *Spectrochim. Acta Part B*, **56**, 2449–2464 (2001).

Encyclopedia of Analytical Chemistry, Online © 2006–2016 John Wiley & Sons, Ltd.

This article was published in the *Encyclopedia of Analytical Chemistry* in 2016 by John Wiley & Sons, Ltd.
DOI: 10.1002/9780470027318.a5107.pub3

57. G.P. Jackson, F.L. King, 'Bulk Plasma Properties in the Pulsed Glow Discharge', *Spectrochim. Acta Part B*, **58**, 1417–1433 (2003).
58. G.P. Jackson, F.L. King, 'Probing Excitation/Ionization Processes in Millisecond Pulsed Glow Discharges in Argon through the Addition of Nitrogen', *Spectrochim. Acta Part B*, **58**, 185–209 (2003).
59. A. Bogaerts, R. Gijbels, G.P. Jackson, 'Modeling of a Millisecond Pulsed Glow Discharge: Investigation of the Afterpeak', *J. Anal. At. Spectrom.*, **18**, 533–548 (2003).
60. A. Bogaerts, 'The Afterglow Mystery of Pulsed Glow Discharges and the Role of Dissociative Electron-Ion Recombination', *J. Anal. At. Spectrom.*, **22**, 502–512 (2007).
61. R.E. Steiner, C.L. Lewis, F.L. King, 'Time-of-flight Mass Spectrometry with a Pulsed Glow Discharge Ionization Source', *Anal. Chem.*, **69**, 1715–1721 (1997).
62. X. Yan, Y. Lin, R. Huang, W. Hang, W.W. Harrison, 'A Spectroscopic Investigation of the Afterglow and Recombination Process in a Microsecond Pulsed Glow Discharge', *J. Anal. At. Spectrom.*, **25**, 534–543 (2010).
63. R. Valledor, J. Pisonero, T. Nelis, N. Bordel, 'Spatial Emission Distribution of a Pulsed Radio-frequency Glow Discharge: Influence of the Pulse Frequency', *Spectrochim. Acta Part B*, **68**, 24–33 (2012).
64. C. Yang, K. Ingeneri, W.W. Harrison, 'A Pulsed Grimm Glow Discharge as an Atomic Emission Source', *J. Anal. At. Spectrom.*, **14**, 693–698 (1999).
65. C. Oxley, W.W. Yang, 'Harrison, Quantitative Depth Analysis using Microsecond Pulsed Glow Discharge Atomic Emission Spectrometry', *J. Anal. At. Spectrom.*, **15**, 1241–1245 (2000).
66. C. Yang, K. Ingeneri, M. Mohill, W.W. Harrison, 'Influence of Discharge Parameters on the Resolution of Depth Profiling by Pulsed Glow Discharge Atomic Emission Spectrometry', *J. Anal. At. Spectrom.*, **15**, 73–78 (2000).
67. R.E. Steiner, C.L. Lewis, V. Majidi, 'Consideration of a Millisecond Pulsed Glow Discharge Time of Flight Mass Spectrometer for Concurrent Elemental and Molecular Analysis', *J. Anal. At. Spectrom.*, **14**, 1537–1541 (1999).
68. V. Majidi, M. Moser, C. Lewis, W. Hang, F.L. King, 'Explicit Chemical Speciation by Microsecond Pulsed Glow Discharge Time-of-flight Mass Spectrometry: Concurrent Acquisition of Structural, Molecular and Elemental Information', *J. Anal. At. Spectrom.*, **15**, 19–25 (2000).
69. S. Canulescu, I.S. Molchan, C. Tauziede, A. Tempez, J.A. Whitby, G.E. Thompson, P. Skeldon, P. Chapon, J. Michler, 'Detection of Negative Ions in Glow Discharge Mass Spectrometry for Analysis of Solid Specimens', *Anal. Bioanal. Chem.*, **396**, 2871–2879 (2010).
70. C.R. Shick, P.A. DePalma, R.K. Marcus, 'Radio-frequency Glow-discharge Mass-spectrometry for the Characterization of Bulk Polymers', *Anal. Chem.*, **68**, 2113–2121 (1996).
71. X.H. Pan, R.K. Marcus, 'Direct Analysis of Glass Powder Samples by Radio-frequency Glow-discharge Atomic Emission Spectrometry (RF-GD-AES)', *Mikrochim. Acta*, **129**, 239–250 (1998).
72. J.A.C. Broekaert, T. Graule, H. Jenett, G. Tolg, P. Tschopel, 'Analysis of Advanced Ceramics and their Basic Products', *Fresenius Z. Anal. Chem.*, **332**, 825–838 (1989).
73. M. Dogar, K. Laqua, H. Massmann, 'Spektrochemische Analysen mit einer Glimmentladungslampe als Lichtquelle-II Analytische Anwengdungen', *Spectrochim. Acta Part B*, **27**, 65–88 (1972).
74. G.S. Lomdahl, R. McPherson, J.V. Sullivan, 'The Atomic Emission Spectrometric Determination of Non-conducting Materials with a Boosted Output Glow-discharge Source', *Anal. Chim. Acta*, **148**, 171–180 (1983).
75. T.J. Loving, W.W. Harrison, 'Dual-pin Cathode Geometry for Glow-discharge Mass-spectrometry', *Anal. Chem.*, **55**, 1526–1530 (1983).
76. S. Caroli, A. Almonti, K. Zimmer, 'Applicability of a Hollow-cathode Emission Source for Determining Trace-elements in Electrically Non-conducting Powders', *Spectrochim. Acta Part B*, **38**, 625–631 (1983).
77. W. Schelles, R.E. Van Grieken, 'Direct Current Glow-Discharge Mass Spectrometric Analysis of Macor Ceramic Using a Secondary Cathode', *Anal. Chem.*, **68**, 3570–3574 (1996).
78. D.M. Wayne, R.K. Schulze, C. Maggiore, D.W. Cooke, G. Havrilla, 'Characterization of Tantalum Films on Analytical Surfaces: Insights into Sputtering of Nonconductors in a Direct-current Glow Discharge Using Secondary Cathodes', *Appl. Spectrosc.*, **53**, 266–277 (1999).
79. W. Schelles, R.E. Van Grieken, 'Quantitative Analysis of Zirconium-oxide by Direct Current Glow-discharge Mass-spectrometry Using a Secondary Cathode', *J. Anal. At. Spectrom.*, **12**, 49–52 (1997).
80. J. Angeli, A. Bengtson, A. Bogaerts, V. Hoffmann, V.-D. Hodoroaba, E. Steers, 'Glow Discharge Optical Emission Spectrometry: Moving towards Reliable Thin Film Analysis – A Short Review', *J. Anal. At. Spectrom.*, **18**, 670–679 (2003).
81. K. Shimizu, H. Habazaki, P. Skeldon, G.E. Thompson, 'Impact of RF-GD-OES in Practical Surface Analysis', *Spectrochim. Acta Part B*, **58**, 1573–1583 (2003).
82. K. Shimizu, H. Habazaki, P. Skeldon, G.E. Thompson, 'Radiofrequency GD-OES: A Powerful Technique for Depth Profiling Analysis of Thin Films', *Surf. Interface Anal.*, **35**, 564–574 (2003).

Encyclopedia of Analytical Chemistry, Online © 2006–2016 John Wiley & Sons, Ltd.

This article was published in the *Encyclopedia of Analytical Chemistry* in 2016 by John Wiley & Sons, Ltd.
DOI: 10.1002/9780470027318.a5107.pub3

83. H. Hocquaux, 'Thin Film Analysis', in *Glow Discharge Spectroscopies*, ed. R.K. Marcus, Plenum Press, New York, 329–372, 1993.
84. A. Bogaerts, R. Gijbels, 'Calculation of Crater Profiles on a Flat Cathode in a Direct Current Glow Discharge, and Comparison with Experiment', *Spectrochim. Acta Part B*, **52**, 765–778 (1997).
85. A. Bogaerts, W. Verscharen, E. Steers, 'Computer Simulations of Crater Profiles in GD-OES: Comparison with Experiments and Investigation of the Underlying Mechanisms', *Spectrochim. Acta Part B*, **59**, 1403–1411 (2004).
86. C.M. Barshick, W.W. Harrison, 'The Laser as an Analytical Probe in Glow-discharge Mass-spectrometry', *Mikrochim. Acta*, **III**, 169–177 (1989).
87. K. Shimizu, H. Habazaki, P. Skeldon, G.E. Thompson, G.C. Wood, 'GDOES Depth Profiling Analysis of Amorphous Ni-P-plated Aluminium Hard Disks', *Surf. Interface Anal.*, **29**, 151–154 (2000).
88. J. Pisonero, C. Perez, R. Pereiro, N. Bordel, A. Sanz-Medel, 'In-depth Profile Analysis by Radiofrequency Glow Discharge Optical Emission Spectrometry using Pressure as Variable Parameter', *J. Anal. At. Spectrom.*, **16**, 370–375 (2001).
89. V. Hoffmann, R. Dorka, L. Wilken, V.-D. Hodoroaba, K. Wetzig, 'Present Possibilities of Thin-layer Analysis by GDOES', *Surf. Interface Anal.*, **35**, 575–582 (2003).
90. R.E. Galindo, R. Gago, D. Duday, C. Palacio, 'Towards Nanometer Resolution in Multilayer Depth Profiling: A Comparative Study of Rutherford Backscattering, Secondary Ion Mass Spectrometry, X-ray Photoelectron Spectroscopy and Glow Discharge Optical Emission Spectrometry', *Anal. Bioanal. Chem.*, **396**, 2725–2740 (2010).
91. L. Lobo, N. Tuccitto, N. Bordel, R. Pereiro, J. Pisonero, A. Licciardello, A. Tempez, P. Chapon, A. Sanz-Medel, 'Polymer Screening by Radiofrequency Glow Discharge Time-of-flight Mass Spectrometry', *Anal. Bioanal. Chem.*, **396**, 2863–2869 (2010).
92. J. Pisonero, A. Licciardello, A. Hierro-Rodriguez, C. Quiros, A. Sanz-Medel, N. Bordel, 'Minor Elements Determination and Evaluation of Diffusion/Segregation Effects on Ultra-thin Layers Using Pulsed Radio-frequency Glow Discharge Time-of-flight Mass Spectrometry', *J. Anal. At. Spectrom.*, **26**, 1604–1609 (2011).
93. P. Sanchez, D. Alberts, B. Fernandez, A. Menendez, R. Pereiro, A. Sanz-Medel, 'Endogenous and Exogenous Hydrogen Influence on Amorphous Silicon Thin Films Analysis by Pulsed Radiofrequency Glow Discharge Optical Emission Spectrometry', *Anal. Chim. Acta*, **714**, 1–7 (2012).
94. B. Fernandez, R. Pereiro, A. Sanz-Medel, 'Glow Discharge Analysis of Nanostructured Materials and Nanolayers – A Review', *Anal. Chim. Acta*, **679**, 7–16 (2010).
95. G. Churchill, K. Putyera, V. Weinstein, X. Wang, E.B.M. Steers, 'New Microsecond-pulsed Direct Current Glow Discharge Assembly on a Fast Flow High Power Source for Time Resolved Analysis in High Resolution Mass Spectrometry', *J. Anal. At. Spectrom.*, **26**, 2263–2273 (2011).
96. C. Engelhard, S.J. Ray, W. Buscher, V. Hoffmann, G.M. Hieftje, 'Correcting Distortion in a Monochromatic Imaging Spectrometer for Application to Elemental Imaging by Glow Discharge Optical Emission Spectrometry', *J. Anal. At. Spectrom.*, **25**, 1874–1881 (2010).
97. G. Gamez, D. Frey, J. Michler, 'Push-broom Hyperspectral Imaging for Elemental Mapping with Glow Discharge Optical Emission Spectrometry', *J. Anal. At. Spectrom.*, **27**, 50–55 (2012).
98. M. Voronov, V. Hoffmann, T. Wallendorf, S. Marke, J. Mönch, C. Engelhard, W. Buscher, S.J. Ray, G.M. Hieftje, Glow Discharge Imaging Spectroscopy with a Novel Acousto-optical Imaging Spectrometer, *J. Anal. At. Spectrom.*, **27**, 419–425 (2012).
99. G. Gamez, M. Voronov, S.J. Ray, V. Hoffmann, G.M. Hieftje, J. Michler, 'Surface Elemental Mapping via Glow Discharge Optical Emission Spectroscopy', *Spectrochim. Acta Part B*, **70**, 1–9 (2012).
100. C.M. Strange, R.K. Marcus, 'Aqueous Sample Introduction into a Glow-discharge Device via a Particle BeamInterface', *Spectrochim. Acta Part B*, **46**, 517–526 (1991).
101. T. Cserfalvi, P. Mezei, P. Apai, 'Emission Studies on a Glow Discharge in Atmospheric Pressure Air using Water as a Cathode', *J. Phys. D Appl. Phys.*, **26**, 2184–2188 (1993).
102. P. Mezei, T. Cserfalvi, 'Electrolyte Cathode Atmospheric Glow Discharges for Direct Solution Analysis', *Appl. Spectrosc. Rev.*, **42**, 573–604 (2007).
103. M.R. Webb, G.C.-Y. Chan, F.J. Andrade, G. Gamez, G.M. Hieftje, 'Spectroscopic Characterization of Ion and Electron Populations in a Solution-cathode Glow Discharge', *J. Anal. At. Spectrom.*, **21**, 525–530 (2006).
104. M.R. Webb, F.J. Andrade, G.M. Hieftje, 'Use of Electrolyte Cathode Glow Discharge (ELCAD) for the Analysis of Complex Mixtures', *J. Anal. At. Spectrom.*, **22**, 766–774 (2007).
105. M.R. Webb, F.J. Andrade, G.M. Hieftje, 'Compact Glow Discharge for the Elemental Analysis of Aqueous Samples', *Anal. Chem.*, **79**, 7899–7905 (2007).
106. M.R. Webb, F.J. Andrade, G.M. Hieftje, 'The Annular Glow Discharge: A Small-scale Plasma for Solution Analysis', *J. Anal. At. Spectrom.*, **22**, 775–782 (2007).
107. Q. He, Z. Zhu, S. Hu, H. Zheng, L. Jin, 'Elemental Determination of Microsamples by Liquid Film Dielectric

Encyclopedia of Analytical Chemistry, Online © 2006–2016 John Wiley & Sons, Ltd.

This article was published in the *Encyclopedia of Analytical Chemistry* in 2016 by John Wiley & Sons, Ltd.
DOI: 10.1002/9780470027318.a5107.pub3

Barrier Discharge Atomic Emission Spectrometry', *Anal. Chem.*, **84**, 4179–4184 (2012).

108. T. Krähling, S. Müller, C. Meyer, A.K. Stark, J. Franzke, 'Liquid Electrode Dielectric Barrier Discharge for the Analysis of Solved Metals', *J. Anal. At. Spectrom.*, **26**, 1974–1978 (2011).
109. S. Tombrink, S. Mueller, R. Heming, A. Michels, P. Lampen, J. Franzke, 'Liquid Analysis Dielectric Capillary Barrier Discharge', *Anal. Bioanal. Chem.*, **397**, 2917–2922 (2010).
110. R.K. Marcus, C.D. Quarles Jr,, C.J. Barringa, A.J. Carado, D.W. Koppenaal, 'Liquid Sampling-atmospheric Pressure Glow Discharge Ionization Source for Elemental Mass Spectrometry', *Anal. Chem.*, **83**, 2425–2429 (2011).
111. T.M. Brewer, J. Castro, R.K. Marcus, 'Particle Beam Sample Introduction into Glow Discharge Plasmas for Speciation Analysis', *Spectrochim. Acta Part B*, **61**, 134–149 (2006).
112. C.D. Quarles Jr,, S. Niemann, R.K. Marcus, 'Conversion of a Commercial GC-MS to a LC-particle Beam/GDMS', *J. Anal. At. Spectrom.*, **25**, 1780–1786 (2010).
113. W.C. Wetzel, F.J. Andrade, J.A.C. Broekaert, G.M. Hieftje, 'Development of a Direct Current He Atmospheric Pressure Glow Discharge as an Ionization Source for Elemental Mass Spectrometry via Hydride Generation', *J. Anal. At. Spectrom.*, **21**, 750–756 (2006).
114. B. Gielniak, T. Fiedler, J.A.C. Broekaert, 'Study of a New Direct Current Atmospheric Pressure Glow Discharge in Helium', *Spectrochim. Acta Part B*, **66**, 21–27 (2011).
115. K. Newman, R.S. Mason, 'Organic Mass Spectrometry and Control of Fragmentation using a Fast Flow Glow Discharge Ion Source', *Rapid Commun. Mass Spectrom.*, **20**, 2067–2073 (2006).
116. K. Fliegel, M. Fuhrer, D. Gonin, 'Günther, Evaluation of a Pulsed Glow Discharge Time-of-flight Mass Spectrometer as a Detector for Gas Chromatography and the Influence of the Glow Discharge Source Parameters on the Information Volume in Chemical Speciation Analysis', *Anal. Bioanal. Chem.*, **386**, 169–179 (2006).
117. R. Meyer, E.L. Heming, U. Gurevich, M. Marggraf, S. Okruss, J. Florek, 'Franzke, Radiofrequency-driven and Low Cost Fabricated Microhollow Cathode Discharge for Gaseous Atomic Emission Spectrometry', *J. Anal. At. Spectrom.*, **26**, 505–510 (2011).
118. C. Meyer, D. Demecz, E.L. Gurevich, U. Marggraf, G. Jestel, J. Franzke, 'Development of a Novel Dielectric Barrier Micro Hollow Cathod Discharge for Gaseous Atomic Emission Spectrometry', *J. Anal. At. Spectrom.*, **27**, 677–681 (2012).
119. J.T. Shelley, G.M. Hieftje, 'Ambient Mass Spectrometry: Approaching the Chemical Analysis of Things as they are', *J. Anal. At. Spectrom.*, **26**, 2153–2159 (2011).
120. J.T. Shelley, G.M. Hieftje, 'Ionization Matrix Effects in Plasma-based Ambient Mass Spectrometry Sources', *J. Anal. At. Spectrom.*, **25**, 345–350 (2010).
121. J. Kratzer, Z. Mester, R.E. Sturgeon, 'Comparison of Dielectric Barrier Discharge, Atmospheric Pressure rf Glow Discharge and DART Sources for Ambient Mass Spectrometry of Acetaminophen', *Spectrochim. Acta Part B*, **66**, 594–603 (2011).
122. J.D. Ingle Jr,, S.R. Crouch, *Spectrochemical Analysis*, Prentice Hall, Englewood Cliffs, NJ, 1988.
123. Y. Talmi, *Multichannel Image Detectors*, ACS Symposium Series 236, American Chemical Society, Washington, DC, Vol. **2**, 1983.
124. Q.S. Hanley, C.W. Earle, F.M. Pennebaker, S.P. Madden, M.B. Denton, 'Charge Transfer Devices in Analytical Instrumentation', *Anal. Chem.*, **68**, 661A–667A (1996).
125. J.H. Giles, T.D. Ridder, R.H. Williams, D.A. Jones, M.B. Denton, 'Selecting a CCD Camera', *Anal. Chem.*, **70**, 663A–668A (1998).
126. E.U. Condon, G.H. Shortley, *The Theory of Atomic Spectra*, Cambridge University Press, Cambridge, 1963.
127. W.F. Meggers, C.H. Corliss, B.F. Scribner, *Tables of Spectral-line Intensities: Part II – Arranged by Wavelengths*, US Government Printing Office, Washington, DC, 1975.
128. J.A.C. Broekaert, 'Atomic Emission Spectroscopy', in *Glow Discharge Spectroscopies*, ed. R.K. Marcus, Plenum Press, New York, 113–174, 1993.
129. E.H. Daughtrey, D.L. Donohue, P.J. Slevin, W.W. Harrison, 'Surface Sputter Effects in a Hollow-cathode Discharge', *Anal. Chem.*, **47**, 683–688 (1975).
130. W.W. Harrison, B.L. Bentz, 'Glow Discharge Mass Spectrometry', *Prog. Anal. Spectrosc.*, **11**, 53–110 (1988).
131. P.F. Little, A. von Engel, 'The Hollow-cathode Effect and the Theory of Glow Discharges', *Proc. R. Soc. London*, **224A**, 209–227 (1954).
132. S.L. Mandelstam, V.V. Nedler, 'On the Sensitivity of Emission Spectrochemical Analysis', *Spectrochim. Acta*, **17**, 885–894 (1961).
133. V. Weinstein, E.B.M. Steers, P. Smid, J.C. Pickering, S. Mushtaq, 'A Detailed Comparison of Spectral Line Intensities with Plane and Hollow Cathodes in a Grimm Type Glow Discharge Source', *J. Anal. At. Spectrom.*, **25**, 1283–1289 (2010).
134. D.S. Gough, 'Direct Analysis of Metals and Alloys by Atomic-absorption Spectrometry', *Anal. Chem.*, **48**, 1926–1931 (1976).
135. A.E. Bernhard, 'Atomic Absorption Spectrometry Using Sputtering Atomization of Solid Samples', *Spectroscopy*, **2**, 24–27 (1987).

Encyclopedia of Analytical Chemistry, Online © 2006–2016 John Wiley & Sons, Ltd.

This article was published in the *Encyclopedia of Analytical Chemistry* in 2016 by John Wiley & Sons, Ltd.
DOI: 10.1002/9780470027318.a5107.pub3

136. A. Walsh, 'The Application of Atomic Absorption Spectra to Chemical Analysis', *Spectrochim. Acta*, **7**, 108–117 (1955).

137. F.L. King Jr,, Quadrupole-based Glow Discharge Mass Spectrometry: Resolution of Polyatomic Ions, PhD Dissertation, University of Virginia, 1989.

138. B.M. Patel, B. Smith, J.D. Winefordner, 'Laser-excited Fluorescence of Diatomic Lead in a Glow-discharge Source', *Spectrochim. Acta Part B*, **40**, 1195–1204 (1985).

139. J.B. Womack, E.M. Gessler, J.D. Winefordner, 'Atomic Fluorescence in a Pulsed Hollow-cathode Discharge with a Copper Vapor Pumped Dye Laser', *Spectrochim. Acta Part B*, **46**, 301–308 (1991).

140. A. Bogaerts, E. Wagner, B.W. Smith, J.D. Winefordner, D. Pollmann, W.W. Harrison, R. Gijbels, 'Three-dimensional Density Profiles of Sputtered Atoms and Ions in a Direct Current Glow Discharge: Experimental Study and Comparison with Calculations', *Spectrochim. Acta Part B*, **52**, 205–218 (1997).

141. A. Bogaerts, R.D. Guenard, B.W. Smith, J.D. Winefordner, W.W. Harrison, R. Gijbels, 'Three-dimensional Density Profiles of the Argon Metastable Atoms in a Direct Current Glow Discharge: Experimental Study and Comparison with Calculations', *Spectrochim. Acta Part B*, **52**, 219–229 (1997).

142. F.M. Penning, 'Demonstration of a New Photoelectric Effect', *Physica*, **8**, 137–140 (1928).

143. C.M. Barshick, R.W. Shaw, J.P. Young, J.M. Ramsey, 'Isotopic Analysis of Uranium Using Glow-discharge Optogalvanic Spectroscopy and Diode Lasers', *Anal. Chem.*, **66**, 4154–4158 (1994).

144. W.A. Mattson, B.L. Bentz, W.W. Harrison, 'Coaxial Cathode Ion-source for Solids Mass Spectrometry', *Anal. Chem.*, **48**, 489–491 (1976).

145. O. Klemperer, *Electron Optics*, Cambridge University Press, Cambridge, 1971.

146. A. Septier, *Focusing of Charge Particles*, Academic Press, New York, 1967.

147. B.L. Bentz, Aspects of Ionization and Sputtering in the Glow Discharge by Solids Mass Spectrometry, PhD Dissertation, University of Virginia, 1980.

148. Etranuclear Laboratories, Inc, *Electrostatic Energy Analyzer Model 616-1 Instruction Manual*, Etranuclear Laboratories, Inc., Pittsburgh, PA, 1977.

149. S.S. Medley, 'Energetic Ion Mass Analysis Using a Radio-frequency Quadrupole Filter', *Rev. Sci. Instrum.*, **49**, 698–706 (1978).

150. W. Paul, H.P. Reinhard, U. VanZahn, 'Das Elektrische Massenfilter als Massenspektrometer und Isotopentrenner', *Z. Phys.*, **152**, 143–182 (1958).

151. M. Szilagyi, *Electron and Ion Optics*, Plenum Press, New York, 1988.

152. H. Wollnik, *Optics of Charged Particles*, Academic Press, Inc., Orlando, 1987.

153. N.R. Daly, 'Scintillation Type Mass Spectrometer Ion Detector', *Rev. Sci. Instrum.*, **31**, 264–267 (1960).

154. F.W. Aston, *Isotopes*, 2nd edition, Longman, New York, 1924.

155. J. Roboz, *Introduction to Mass Spectrometry: Instrumentation and Techniques*, Interscience, New York, 1968.

156. A.A. Rubinshtein, G.D. Schilling, S.J. Ray, P.P. Sperline, M.B. Denton, C.J. Barinaga, D.W. Koppenaal, G.M. Hieftje, 'Characterization of a Third-generation Faraday-strip Array Detector Coupled to a Mattauch-Herzog Geometry Mass Spectrograph with a dc GD Ionization Source', *J. Anal. At. Spectrom.*, **25**, 735–738 (2010).

157. R.S. Houk, 'Mass-spectrometry of Inductively Coupled Plasmas', *Anal. Chem.*, **58**, 97A–105A (1986).

158. P.H. Dawson, *Quadrupole Mass Spectrometry and its Applications*, Elsevier Scientific, New York, 1976.

159. M.V. Buchanan, R.L. Hettich, 'Fourier-transform Mass-spectrometry of High-mass Biomolecules', *Anal. Chem.*, **65**, 245A–259A (1993).

160. S.A. McLuckey, G.J. Van Berkel, D.E. Goeringer, G.L. Glish, 'Ion-trap Mass-spectrometry of Externally Generated Ions', *Anal. Chem.*, **66**, 689A–696A (1994).

161. A.G. Marshall, P.B. Grosshans, 'Fourier-transform Ion-cyclotron Resonance Mass-spectrometry: the Teenage Years', *Anal. Chem.*, **63**, 215A–229A (1991).

162. N.M.M. Nibbering, 'Gas-phase Ion Molecule Reactions as Studied by Fourier-transform Ion-cyclotron Resonance', *Acc. Chem. Res.*, **23**, 279–285 (1990).

163. D.C. Duckworth, C.M. Barshick, 'Ion Traps: What do they Hold for Elemental Analysis', *Anal. Chem.*, **70**, 709A–717A (1998).

164. M.B. Comisarow, A.G. Marshall, 'Theory of Fourier-transform Ion-cyclotron Resonance Mass-spectrometry 1. Fundamental Equations and Low Pressure Line-shape', *J. Chem. Phys.*, **64**, 110–119 (1976).

165. W.W. Harrison, W. Hang, 'Pulsed Glow Discharge Time-of-flight Mass Spectrometry', *J. Anal. At. Spectrom.*, **11**, 835–840 (1996).

166. R. Pereiro, A. Sola-Vazquez, L. Lobo, J. Pisonero, N. Bordel, J.M. Costa, A. Sanz-Medel, 'Present and Future of GD-TOF-MS in Analytical Chemistry', *Spectrochim. Acta Part B*, **66**, 399–412 (2011).

167. S. Mushtaq, J.C. Pickering, E.B.M. Steers, P. Horvath, J.A. Whitby, J. Michler, 'The Role of Oxygen in Analytical Glow Discharges: GD-OES and GD-TOF-MS Studies', *J. Anal. At. Spectrom.*, **26**, 1746–1755 (2011).

Encyclopedia of Analytical Chemistry, Online © 2006–2016 John Wiley & Sons, Ltd.

This article was published in the *Encyclopedia of Analytical Chemistry* in 2016 by John Wiley & Sons, Ltd.
DOI: 10.1002/9780470027318.a5107.pub3